# IMPACT OF DESIGN VARIABLES ON SEISMIC FRAGILITY OF BRIDGES IN GEORGIA

A Thesis
Presented to
The Academic Faculty

by

Piyush Sood

In Partial Fulfillment
of the Requirements for the Degree
Master of Science in Civil Engineering in the
School of Civil and Environmental Engineering

Georgia Institute of Technology
December 2017

**COPYRIGHT © 2017 BY PIYUSH SOOD**

# IMPACT OF DESIGN VARIABLES ON SEISMIC FRAGILITY OF BRIDGES IN GEORGIA

Approved by:

Dr. Iris Tien, Advisor
School of Civil and Environmental Engineering
*Georgia Institute of Technology*

Dr. Reginald DesRoches
William and Stephanie Sick Dean of the George R. Brown School of Engineering
*Rice University*

Dr. Chuang-Sheng (Walter) Yang
School of Civil and Environmental Engineering
*Georgia Institute of Technology*

Date Approved: August 22, 2017

To my parents for their love and support

# ACKNOWLEDGEMENTS

I would like to thank my research supervisors Dr. Iris Tien, Dr. Reginald DesRoches, and Dr. Chuang-Sheng (Walter) Yang. Without their assistance and involvement throughout the process, this thesis would have never been accomplished. I discussed early versions of the thesis with Dr. Yang, and he raised many vital points in our discussions. I hope that I have managed to address several of them in my work.

I would like to express gratitude to my research partners, Albert Zhang and Borja Zarco, for collaborating with me to make my work.

I would also like to thank my previous advisor, Dr. Jayadipta Ghosh, who introduced me to the field of probabilistic structural analysis of bridges and laid a strong foundation for my current research.

I would also like to thank my parents and friends, especially Shreya, Shivang and Avion for their encouragement to complete this work. Their help and support have made the project possible. Finally, I am most grateful to my parents, who offered their encouragement through phone calls, despite my own limited devotion to correspondence. Nobody can achieve their dreams alone, so therefore, to all that have helped me, I am overwhelmingly grateful.

# TABLE OF CONTENTS


**ACKNOWLEDGEMENTS** iv

**LIST OF TABLES** vii

**LIST OF FIGURES** x

**SUMMARY** xiii

**CHAPTER 1. Introduction** 1
**1.1 Problem Description** 1
**1.2 Objectives and Scope of Research** 3
**1.3 Thesis Outline** 4

**CHAPTER 2. Lap Splice Formulation and Parametric Study** 6
**2.1 Introduction** 6
**2.2 Literature Review** 8
**2.3 Lap Splice Formulation** 11
**2.4 Effects of variables on Splice Strength** 16
2.4.1 Effect of Lap Splice Length 16
2.4.2 Effect of Transverse Reinforcement 18
2.4.3 Effect of Steel Yield Strength 20
2.4.4 Effect of Rebar Diameter 21

**CHAPTER 3. Georgia Seismic Hazard maps and Bridge Inventory Analysis** 24
**3.1 Georgia Design Response Spectrum** 24
3.1.1 Seismic Zones 30
**3.2 Georgia Site-Specific Seismic Hazard Maps** 31
3.2.1 Site Class A Seismic Hazard Map 32
3.2.2 Site Class B Seismic Hazard Map 33
3.2.3 Site Class C Seismic Hazard Map 33
3.2.4 Site Class D Seismic Hazard Map 34
3.2.5 Site Class E Seismic Hazard Map 35
**3.3 Georgia Highway Bridge Inventory Analysis** 35
3.3.1 Bridge Class Statistics 38

**CHAPTER 4. Overview of Fragility Curves** 41
**4.1 Analytical Fragility Curve Formulation** 41
4.1.1 Component-Level Fragility Curves 44
4.1.2 System-Level Fragility Curves 44
**4.2 Limit States** 46
4.2.1 Columns 48
**4.3 Probabilistic Seismic Demand Model** 51

**CHAPTER 5. MODELING and Deterministic Seismic Bridge Analyses** 52
**5.1 Typical Highway Bridge Components** 52

**5.2 Deterministic Seismic Response 54**
5.2.1 Multi-Span Simply Supported Concrete Girder Bridge 54
5.2.2 Multi-Span Continuous Steel Girder Bridge 61
5.2.3 Multi-Span Simply Supported Steel Girder Bridge 66

**CHAPTER 6. Site-Specific Fragility Curves 70**
**6.1 PSDMs for Multi-Span Highway Bridges 70**
**6.2 Seismic Fragility Curves and Site Specific Risk Estimates 71**
6.2.1 Multi-Span Simply Supported Concrete Bridges 72
6.2.2 Multi-Span Continuous Steel Bridges 79
6.2.3 Multi-Span Simply Supported Steel Bridges 85

**CHAPTER 7. Conclusions, key contributions and future work 94**
**7.1 Summary and Key Contributions 94**
**7.2 Future Work 98**

**REFERENCES 100**

# LIST OF TABLES

Table 3-1 – Values of Site Factor, $F_{PGA}$, at Zero Period on Acceleration Spectrum (AASHTO, 2014). ..... 28

Table 3-2 – Values of Site Factor, $F_a$, for Short Period Range of Acceleration Spectrum (AASHTO, 2014). ..... 28

Table 3-3 – Values of Site Factor, $F_v$, for Long Period Range of Acceleration Spectrum (AASHTO, 2014). ..... 28

Table 3-4 – Seismic Zone Boundaries. ..... 31

Table 3-5 – Georgia Highway Bridges Classified as per Their Construction Material (FHWA, 2002). ..... 37

Table 3-6 – Georgia Highway Bridges Classified as per Their Construction Type (FHWA 2002). ..... 37

Table 3-7 – Georgia Bridge Classes and Their Proportions (FHWA 2002). ..... 38

Table 3-8 – Span Number Statistics for Four Bridge Classes Considered. ..... 39

Table 3-9 – Maximum Span Length Statistics for Four Bridge Classes. ..... 39

Table 3-10 – Deck Width Statistics for Four Bridge Classes. ..... 40

Table 3-11 – Minimum Vertical Deck Width Statistics for Four Bridge Classes. ..... 40

Table 4-1 – HAZUS' Qualitative Limit States (FEMA, 2003). ..... 47

Table 4-2 – Limit State Median Values for Lap Spliced Column Sections. ..... 50

Table 6-1 – Comparative Probability Estimates of Exceeding Four Limit States for MSSS Concrete Bridges for (a) No-Lap Splice with Seismic Spacing (s = 3 in.), (b) Lap Splice with Seismic Spacing (s = 3 in.), and (c) Lap Splice with Seismic Spacing (s = 12 in.). ..... 73

Table 6-2 – Seismic Risk for MSSS Concrete Bridges for Site Class A when Lap-Splice with Non-Seismic Spacing is Provided. ..... 74

Table 6-3 – Seismic Risk for MSSS Concrete Bridges for Site Class B when Lap-Splice with Non-Seismic Spacing is Provided. ..... 75

Table 6-4 – Seismic Risk for MSSS Concrete Bridges for Site Class C when (a) Lap-Splice with Non-Seismic Spacing is Provided, (b) Lap-Splice with Seismic Spacing is Provided, and (c) No Lap Splice is Provided.....76

Table 6-5 – Seismic Risk for MSSS Concrete Bridges for Site Class D when (a) Lap-Splice with Non-Seismic Spacing is Provided, (b) Lap-Splice with Seismic Spacing is Provided for Zone 1-B and No Lap Splice is Provided for Zone 2.....77

Table 6-6 – Seismic Risk for MSSS Concrete Bridges for Site Class E when (a) Lap-Splice with Non-Seismic Spacing is Provided, (b) Lap-Splice with Seismic Spacing is Provided for Zone 1-B and No Lap Splice is Provided for Zone 2.....78

Table 6-7 – Comparative Probability Estimates of Exceeding Four Limit States for MSC Steel Bridges for (a) No-Lap Splice with Seismic Spacing (s = 3 in.), (b) Lap Splice with Seismic Spacing (s = 3 in.), and (c) Lap Splice with Seismic Spacing (s = 12 in.). .....80

Table 6-8 – Seismic Risk for MSC Steel Bridges for Site Class A when Lap-Splice with Non-Seismic Spacing is Provided.....81

Table 6-9 – Seismic Risk for MSC Steel Bridges for Site Class B when (a) Lap-Splice with Non-Seismic Spacing is Provided, (b) Lap-Splice with Seismic Spacing is Provided, and (c) No Lap Splice is Provided.....82

Table 6-10 – Seismic Risk for MSC Supported Steel Bridges for Site Class C when (a) Lap-Splice with Non-Seismic Spacing is Provided, (b) Lap-Splice with Seismic Spacing is Provided, and (c) No Lap Splice is Provided. .....83

Table 6-11 – Seismic Risk for MSC Steel Bridges for Site Class C when (a) Lap-Splice with Non-Seismic Spacing is Provided, and (b) No Lap Splice is Provided. .....84

Table 6-12 – Seismic Risk for MSC Steel Bridge Class for Site Class C when (a) Lap-Splice with Non-Seismic Spacing is Provided, and (b) No Lap Splice is Provided.....85

Table 6-13 – Comparative Probability Estimates of Exceeding Four Limit States for MSSS Steel Bridges for (a) No-Lap Splice with Seismic Spacing (s = 3 in.), (b) Lap Splice with Seismic Spacing (s = 3 in.), and (c) Lap Splice with Seismic Spacing (s = 12 in.). .....88

Table 6-14 – Seismic Risk for MSSS Steel Bridges for Site Class A when Lap-Splice with Non-Seismic Spacing is Provided.....89

Table 6-15 – Seismic Risk for MSSS Steel Bridges for Site Class B when (a) Lap-Splice with Non-Seismic Spacing is Provided, (b) Lap-Splice with Seismic Spacing is Provided, and (c) No Lap Splice is Provided.....90

Table 6-16 – Seismic Risk for MSSS Steel Bridges for Site Class C when (a) Lap-Splice with Non-Seismic Spacing is Provided, (b) Lap-Splice with Seismic Spacing is Provided, and (c) No Lap Splice is Provided. ..... 91

Table 6-17 – Seismic Risk for MSSS Steel Bridges for Site Class C when (a) Lap-Splice with Non-Seismic Spacing is Provided, and (b) No Lap Splice is Provided. ..... 92

Table 6-18 – Seismic Risk for MSSS Steel Bridges for Site Class C when (a) Lap-Splice with Non-Seismic Spacing is Provided, and (b) No Lap Splice is Provided ..... 93

# LIST OF FIGURES

Figure 2.1 – Column Failure leading to Collapse of Substructure Collapse of Cypress Viaduct in Oakland, California. ..... 7

Figure 2.2 – Overturning Failure of Bridge Segment on Hanshin Expressway due to Inadequate Transverse Reinforcement, Improper Longitudinal Reinforcement Anchorage and Soil-Structure Interactions. ..... 8

Figure 2.3 – Test Setup Used by Melek and Wallace (2004) for Lateral Cyclic Loading of Columns. ..... 10

Figure 2.4 – Stress-Strain Curve for Lap Splice Model ..... 13

Figure 2.5 – Fictitious Characteristic Block for (a) Circular and (b) Square Column... 14

Figure 2.6 – Lap Splice Stress-Strain Plot for Commonly Used Splice Lengths of 6.5 ft. and 9 ft. in Georgia. ..... 17

Figure 2.7 – Effect of Change in Lap Splice Length on Peak and Residual Stress of Spliced Section. ..... 18

Figure 2.8 – Lap Splice Stress-Strain Plot for Commonly Used Transverse Spacing of 12 in Georgia. ..... 19

Figure 2.9 – Effect of Change in Transverse Reinforcement Spacing on Peak and Residual Stress of Spliced Section. ..... 20

Figure 2.10 – Lap Splice Stress-Strain Plot for Commonly Used Steels in Georgia..... 21

Figure 2.11 – Effect of Change in Steel Yield Strength on Peak and Residual Stress of Spliced Section. ..... 21

Figure 2.12 – Lap Splice Stress-Strain Plot for Commonly Used #11 Rebar in Georgia. ..... 22

Figure 2.13 – Effect of Change in Longitudinal Rebar Diameter on Peak and Residual Stress of Spliced Section. ..... 23

Figure 3.1 – Map of Georgia Depicting Contour Lines for Seismic Site Class B for (a) Horizontal Peak Ground Acceleration (PGA) Coefficient; (b) Horizontal Response Spectral Acceleration Coefficient at Period 0.2 Seconds ($S_S$); and (c) Horizontal Response Spectral Acceleration Coefficient at Period 1.0 Second ($S_1$) (AASHTO, 2014). ..... 26

Figure 3.2 – Design Response Spectrum (AASHTO, 2014) .....27

Figure 3.3 – Georgia Design Response Spectra for Site Classes A, B, C, D and E.....29

Figure 3.4 – Spectral Acceleration Plot for a Range of Time Periods for the 48 Rix and Fernandez Ground Motion Suite. .....30

Figure 3.5 – The Map of Georgia Showing Six Zones Considered in the Study. .....32

Figure 3.6 – Georgia Seismic Hazard Map for Site Class A .....32

Figure 3.7 – Georgia Seismic Hazard Map for Site Class B.....33

Figure 3.8 – Georgia Seismic Hazard Map for Site Class C.....34

Figure 3.9 – Georgia Seismic Hazard Map for Site Class D .....34

Figure 3.10 – Georgia Seismic Hazard Map for Site Class E.....35

Figure 4.1 – Typical Fragility Curve .....42

Figure 4.2 – Moment-Curvature Ductility Curves and Limit States for: (a) Column with No Lap Splice and Non-Seismic Transverse Detailing; (b) Column with Lap Splice and Non-Seismic Transverse Detailing; and (c) Column with Lap Splice and Seismic Transverse Detailing. .....50

Figure 5.1 – Typical Bridge Configuration.....53

Figure 5.2 – Acceleration-Time Plot for Rix Ground Motion Selected for Deterministic Bridge Analysis. .....54

Figure 5.3 – Multi-Span Simply Supported Concrete Girder Bridge Layout. .....55

Figure 5.4 – Cross-Sectional Layout for Bent Beam and Column for Multi-Span Simply Supported Concrete Girder Bridge. .....56

Figure 5.5 – Typical Layout of Elastomeric Bearing.....57

Figure 5.6 – Stress-Strain Model Used for (a) Elastomeric Pad, and (b) Dowel Bar in the Elastomeric Bearing. .....59

Figure 5.7 – Curvature Demand on Column Base of MSSS Concrete Bridge. .....60

Figure 5.8 – Force-Displacement Curves for (a) Fixed (b) Expansion Laminated Elastomeric Bearings Used in MSSS Concrete Bridge.....61

Figure 5.9 – Multi-Span Continuous Steel Girder Bridge Layout. .....62

Figure 5.10 – Cross-Sectional Layout for Bent Beam and Column for Multi-Span Continuous Steel Girder Bridge. ..... 63

Figure 5.11 – Typical Layout of Low-Profile Steel Fixed Bearing ..... 63

Figure 5.12 – Curvature Demand on Column Base of MSC Steel Girder Bridge. ..... 65

Figure 5.13 – Force Force-Displacement Curves for (a) Fixed (b) Expansion Steel Bearings Used in MSC Steel Girder Bridge. ..... 66

Figure 5.14 – Multi-Span Simply Supported Steel Girder Bridge Layout. ..... 67

Figure 5.15 – Cross-Sectional Layout for Bent Beam and Column for Multi-Span Simply Supported Steel Girder Bridge. ..... 68

Figure 5.16 – Curvature Demand on Column Base of MSSS Steel Girder Bridge. ..... 68

Figure 5.17 - Force-Displacement Curves for (a) Fixed (b) Expansion Steel Bearings Used in MSSS Steel Girder Bridge. ..... 69

Figure 6.1 – Probabilistic Seismic Demand Models (PSDMs) for Column Curvature Ductility Demand for (a) MSSS Concrete Bridge, (b) MSC Steel Girder Bridge, and (c) MSSS Steel Girder Bridge ..... 71

Figure 6.2 – Seismic Fragility Curves for MSSS Concrete Class for (a) No-Lap Splice with Seismic Spacing (s = 3 in.), (b) Lap Splice with Seismic Spacing (s = 3 in.), and (c) Lap Splice with Seismic Spacing (s = 12 in.). ..... 72

Figure 6.3 - Seismic Fragility Curves for MSC Steel Class for (a) No-Lap Splice with Seismic Spacing (s = 3 in.), (b) Lap Splice with Seismic Spacing (s = 3 in.), and (c) Lap Splice with Seismic Spacing (s = 12 in.). ..... 79

Figure 6.4 - Seismic Fragility Curves for MSSS Steel Bridges for (a) No-Lap Splice with Seismic Spacing (s = 3 in.), (b) Lap Splice with Seismic Spacing (s = 3 in.), and (c) Lap Splice with Seismic Spacing (s = 12 in.). ..... 87

# SUMMARY

The state of Georgia is identified as a region with low-to-moderate seismic activity. Most bridges in the state have been designed to resist moderate earthquake loads. However, recent seismological studies performed for Georgia Department of Transportation (GDOT) have shown that there are a few bridge types that may warrant further review, depending on their dynamic characteristics, local soil conditions, and ground motion frequency contents. Three of the most common factors for the deficiency in performance in a possible seismic event arise from lap splice at column bases, inadequate transverse reinforcement configurations, and insufficient embedded length of piles into bents or pile-to-bent reinforcement development.

In this study, the performance of representative bridges from different classes in Georgia is investigated to estimate their expected seismic behavior considering the latest AASHTO LRFD Design Specifications. The responses are compared with the previously used design practices in the Georgia's Bridge and Structure Design Manual. Different cases of lap splice lengths, seismic and non-seismic spacing, and seismic and non-seismic pile bents are compared by the means of nonlinear time history analyses. Probabilistic analysis is accomplished through analyzing these bridges under a suite of 48 ground motions to compare the component capacity against the imposed demand of the columns and piles. Seismic damage risk estimates computed through the probabilistic analyses for different seismic site classes and for different regions in the state are used to make important recommendations on the bridges to be built in the future.

# CHAPTER 1. INTRODUCTION

## 1.1 Problem Description

The seismic provisions were introduced in the AASHTO LRFD Bridge Design Specifications after several bridges built before 1970s suffered severe damage and collapse. These bridges were unable to withstand even earthquakes of modern intensities due to inadequate seismic capacity of concrete columns. While earthquakes are considered primarily a west coast problem, geologists have observed ongoing tectonism in southeastern region as well (Biryol et al., 2016). In fact, the southeastern US has seen some of the biggest earthquakes in the history, e.g. the New Madrid earthquake, the Charleston earthquake, etc. Because Georgia lies in the vicinity of this active seismic region, a low-to-moderate seismic hazard is identified in the state. Recent studies have shown that seismic risk in Georgia, even though low, can impose significant demands on some bridges depending on their dynamic characteristics (Hite, 2007). This led to the adoption of seismic provisions of AASTHO LRFD Design Specifications (2014) into Georgia's Bridge and Structures Design Manual (GDOT, 2017). With this regard, there is a considerable need to evaluate the seismic performance and associated damage risk of Georgia's previously built highway bridges. Studying the impact of the latest developments in the LRFD Specifications on these structures allows the identification of what developments are resolving the issue, what interventions can be improved upon, and what new developments may need to be made.

The latest AASHTO LRFD Design Specifications (2014) recognize the seismic hazard return period to be equal to 1000 years instead of previously adopted return period

of 500 years which has resulted in a shift of boundaries of seismic performance zones. According to the latest code, the upper boundary for spectral acceleration (at 1.0 second) for Seismic Zone I is 0.15 as opposed to 0.10 in the previous AASTHO Specifications (2011). The code has special seismic design requirements defined for Seismic Zones II, III and IV, however, the change in the spectral acceleration boundaries has led to some ambiguity regarding the lap splice and transverse detailing requirements for Seismic Zone I when the spectral acceleration is between 0.10 and 0.15.

Lap splices are an essential part of reinforced concrete structures as they help to maintain the continuity between the structural members. In the past, it has been customary to provide lap splices at the bottom of the bridge columns to maintain continuity of the connection with the foundations. During earthquake events, column connections with other bridge components, such as foundations and bent caps, are subjected to significant moments that lead to tensile stresses in the longitudinal reinforcement. If a lap splice is present at these locations, it results in splitting bond failure due to stiffness degradation and low deformation capacity (Jaradat, McLean, and Marsh, 1998; Lin and Hawkins, 1996). Furthermore, inadequate lap splice length complemented with widely spaced transverse reinforcement worsens the seismic performance of these columns. Adequate transverse confinement is necessary to develop a bond between longitudinal bars and surrounding concrete, so that the transfer of force between the two spliced bars happens effectively. Previous research has shown that the lack of adequate transverse reinforcement leads to low flexural strength, low shear strength and low ductility, which results in a higher damage risk.

In the recent decades, seismic fragility curves have been used extensively to evaluate the damage risk associated with bridge components and the structure as a whole (J. B. Mander and Basöz, 1999; Nielson, 2005; B. Nielson and DesRoches, 2007; Ghosh and Padgett, 2010). Fragility curves depict the conditional probability of a structural component reaching or exceeding a limit state given the intensity measure of the earthquake. Ranging from rudimentary to hybrid methods, researchers have developed several ways to quantify the vulnerability of structures. Analytical fragility curves are utilized in this study to assess the impact of latest AASHTO Design Specifications on highway bridges in Georgia. These curves are used to estimate the associated seismic damage risk as a function of seismic hazard levels in various regions in the state.

## 1.2 Objectives and Scope of Research

The goal of the research is to evaluate the seismic performance and fragility of existing multi-span highway bridge classes in Georgia considering the latest AASTHO LRFD seismic design provisions. Based on the results, the study aims to provide recommendations to Georgia Department of Transportation (GDOT) about lap splice requirements and seismic detailing for multi-span bridges to be built in future.

The following are the specific tasks that will be completed in this research:

1. Review commonly used detailing practices in Bridge and Structures Design Manual (GDOT, 2017) in the current design codes and compare them with the latest seismic design provisions in AASHTO LRFD Design Specification (2014).

2. Complete a literature review on the previous research done on lap splices; develop a stress-strain curve for the lap spliced section based on the truss-based force transfer mechanism model to evaluate its impact on columns.

3. Develop seismic hazard maps and design response spectra for various regions in the state of Georgia to estimate the expected peak ground accelerations in these regions.

4. Develop three-dimensional analytical models of selected multi-span bridges by carefully studying the bridge plans and incorporating the previously developed lap splice models to assess their seismic performance.

5. Perform deterministic seismic analysis considering the current practices used in Georgia and the latest AASHTO LRFD to assess the performance differences between the two design codes.

6. Generate probabilistic seismic demand models and fragility curves as a function of lap splice length and transverse reinforcement spacing to estimate the associated seismic damage risk.

7. Provide recommendations to Georgia Department of Transportation (GDOT) for the bridges to be built in future based on the obtained results.

## 1.3 Thesis Outline

The thesis is organized into 7 chapters:

Chapter 2 presents an overview of past research conducted on lap splices highlighting the importance of providing adequate lap splice and transverse reinforcement especially in

columns in seismically active regions. Furthermore, this chapter also presents the stress-strain formulation used to study the lap splice behavior and effects of various geometric parameters on the lap splice strength.

Chapter 3 presents potential seismic hazard for Site Classes A, B, C, D and E in the state of Georgia. The state is divided into 6 regions based on the potential peak ground acceleration in these regions. This chapter further provides a brief overview of bridge inventory in the state of Georgia.

Chapter 4 summarizes the mathematical framework employed to formulate the analytical fragility curves in the study, along with the limit state capacity and probabilistic seismic demand model definitions.

Chapter 5 presents the characteristics of the representative bridge class for each of the three bridge classes, namely multi-span simply supported concrete girder bridges, multi-span continuous steel girder bridges and multi-span simply supported steel girder bridges, analyzed in the study. This chapter further explores the effect of lap splice and transverse reinforcement spacing on the columns and bearings of the bridge.

Chapter 6 presents the seismic fragility curves for each of the bridge classes. It further evaluates the site-specific fragility damage risk estimates for columns to determine the appropriate lap splice and detailing requirement for various regions in the state of Georgia.

Finally, Chapter 7 presents the key contributions of the research along with recommendations for the future work.

# CHAPTER 2. LAP SPLICE FORMULATION AND PARAMETRIC STUDY

Studies on lap splices began in the mid-1970s when several bridge columns suffered severe damage and collapse during moderate intensity earthquakes. Researchers conducted experimental tests to investigate the impact of lap splice lengths and transverse detailing on column strength and ductility. This chapter gives the summary of these studies and highlights the importance of providing splice lengths and transverse detailing on column strength and ductility. In the second section, the chapter presents a lap splice formulation that is used in for assessing the bridge fragility curves. Finally, a parametric study is presented to investigate the effect of variables that effect the strength of a lap spliced section.

## 2.1 Introduction

This study focusses on seismic evaluation of highway bridges located in the state of Georgia as most of these bridges were built with very little or no seismic considerations with typical deficiency characterized by presence of lap splice at the column bases and inadequate transverse reinforcement. Situated in a moderate intensity seismic activity region, old bridges in Georgia face a risk of partial or complete damage due in a possible earthquake event.

The above-mentioned factors were identified as a threat to bridges built before 1970. The first instance of the need of the seismic detailing was recognized in the San Fernando earthquake. Despite being considered an earthquake of moderate intensity, it led to the

collapse of five freeways. More recent examples include the upper deck failure of the Cypress viaduct of Interstate 880 after the Loma Prieta Earthquake in 1989. As shown in Figure 2.1, the columns of the viaduct could not support the superstructure leading to the death of 42 people by falling roadway. Most of the other bridges collapsed in the Loma Prieta earthquake were constructed before 1971 and lacked seismic detailing requirements (Zhiqiang and Lee, 2009).


**Figure 2.1 – Column Failure leading to Collapse of Substructure Collapse of Cypress Viaduct in Oakland, California.**

A similar type of failure was also identified in the 1995 Kobe earthquake in which a 630m intermediate segment of the Hanshin Expressway supported by 18 circular columns failed as shown in Figure 2.2. Post-earthquake investigations revealed that poor transverse column reinforcement, improper anchorage of longitudinal reinforcement and lack of study of soil-structure interactions lead to overturning of the complete bridge in the transverse direction (Mylonakis et. al., 2006). It was also found that the longitudinal reinforcement bars joined together using butt welding at the base of the columns lacked flexural strength which was a cause of failure.

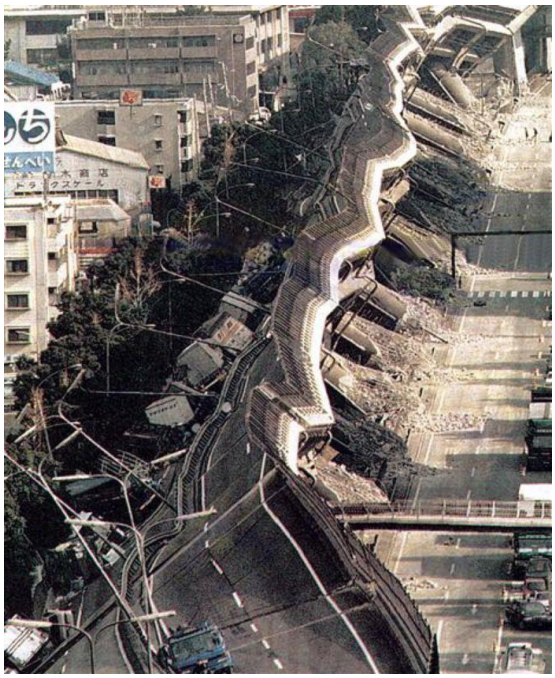

**Figure 2.2(a)**

**Figure 2.2(b)**

**Figure 2.2 – Overturning Failure of Bridge Segment on Hanshin Expressway due to Inadequate Transverse Reinforcement, Improper Longitudinal Reinforcement Anchorage and Soil-Structure Interactions.**

The substructure for any bridge plays an important role in transferring all types of loads imposed on the bridge to the ground. Failure of seismically inadequate columns has led to severe damage or collapse of bridges in the past. This warrants a detailed review of column detailing in Georgia to make columns and bridges safer.

## 2.2 Literature Review

The earliest experimental research was conducted by Orangun, Jirsa, and Breen (1977) who developed an empirical design equation for development and lap splice length in terms of steel stress, concrete strength, bar diameter, concrete cover, and transverse reinforcement. This equation was later adopted into the 1989 ACI Building Codes. Later,

these equations were revised by experimental tests carried out by Sozen and Moehle (1990).

In the same decade, Cairns and Arthur (1979) carried out an experimental test in which they evaluated responses from 51 columns with smooth and roughened longitudinal bars under lateral cyclic loading. The most important conclusion from this research was that lap spliced sections in tension and compression have significantly different responses. Furthermore, they revealed that the columns with roughened bars performed significantly better than the columns with smooth bars.

Studies by Paulay et. al. (1981) revealed the importance of confinement by transverse reinforcement in spliced column sections. They performed experimental tests on 12 specimens and found that despite of insufficient lap splice length, well-confined columns could develop tensile yield stress in the longitudinal reinforcement and maintain their lateral load capacity up to high displacement ductility of about 4.

Lynn et. al. (1996) investigated the impact of longitudinal reinforcement ratio and transverse spacing on lap-spliced columns from the pre-1970s. The test specimens included eight 18 inch square columns out of which five had continuous reinforcement and three has lap splices at the bottom of the columns. These columns were subjected to reversed cyclic lateral displacements under a vertical load. The findings of the research revealed that the columns with a low reinforcement ratio subjected to low axial stresses showed a ductile response with a displacement ductility up to 4.2, however, ultimately the columns with a lap splice failed in shear due to cracks developed along the lap splice. On the other hand,

the columns subjected to high axial stresses showed brittle failure irrespective of the presence of a lap splice shorty after reaching he yield strength.

Melek and Wallace (2004) also conducted a similar study to examine the effects of lap-splices on short columns through experimental tests. The columns in their experiments were subjected to lateral cyclic loading while under axial compression as shown in Figure 2.3. Their findings revealed that inadequate confining reinforcement led to bond deterioration between reinforcement bars and surrounding concrete. This led to steep degradation in the strength of columns at lateral drift ratios of 1.0% to 1.5%. Later, Cho and Pincheira (2004) proposed an analytical modelling approach using different bond slip relationships to match the experimental results by Melek and Wallace (2004).

**Figure 2.3 – Test Setup Used by Melek and Wallace (2004) for Lateral Cyclic Loading of Columns.**

Another study to investigate the effect of lap splices on beams was conducted by Harajli et. al. (2005). They evaluated the stress strain relationship based on the bond-slip behavior between steel and concrete when the beams were subjected to four-point flexural test with the lap splice in the middle. In a similar study, Wu et al. (2013) conducted a

similar study on lap-spliced beam sections with enamel coated reinforcing bars and found that enamel coating increases the bond strength of deformed rebars in normal strength concrete.

Recently, studies have also been conducted to evaluate the response of lap spliced sections in high strength concrete members (Hamad and Najjar 2002; El-Azab, Mohamed, and Farahat 2014; Mabrouk and Mounir 2017). These studies show a similar response as earlier ones and highlight the importance of adequate lap splice lengths and transverse detailing for better column performance. While all these studies mostly focus on the strength evaluation in the lap splice sections, several studies have been carried out to improve the strength of lap spliced columns and beams through steel and FRP jacketing (Aboutaha et al. 1996; Biskinis and Fardis 2007; M. H. Harajli and Dagher 2008)

All these studies reveal a significant need of adequate lap splice length and transverse detailing to better the response of columns under lateral cyclic loading. The objective of this study is to assess these details for previously built highway bridges in Georgia and compare them with the latest AASHTO Design Specifications by the means of fragility curves.

## 2.3 Lap Splice Formulation

Force transfer phenomenon in a lap-spliced section follows a complex mechanism, however, simplifications have been made based on basic mechanistic principles to simulate its behavior. Traditionally, two mechanisms have been used to model this behavior: bond mechanism and truss mechanism (Hannewald, 2013). In a structural member, both

mechanisms act together, however, for modelling purposes, it is fair to assume that either of the mechanisms dominates.

The basic principle of the bond mechanism follows that the lugs on the reinforcement bar exert a bearing force on the surrounding concrete at an angle. The component of this force parallel to the axis of the rebar causes shearing stress in the concrete, and the normal component of this force exerts a radial stress on concrete causing splitting of concrete. When the resultant stress exceeds the tensile capacity of concrete, concrete is no longer able to take the bearing force exerted by reinforcement lugs and hence, failure of the section occurs.

On the other hand, in the truss mechanism, a simple truss model is used to calculate the force transfer between the lap-spliced bars and surrounding concrete. Priestley (1996) proposed the truss system methodology to model the approximate response of the longitudinal reinforcement in a lap-spliced section in tension. Tariverdilo et. al (2009) used the truss mechanism model to evaluate the fragility functions for reinforced concrete (RC) frames with lap spliced columns and matched the results with the experimental work done by Aboutaha et al. (1996) and Melek et al. (2004). They concluded that the truss model adequately captures the maximum strength and post peak softening behavior of spliced sections. Canbay et al. (2005) suggested a similar approach to evaluate the lap splice behavior, however, their model also included some empirical factors. The model used in this study is purely based on theory and identical to model suggested by Priestley (1996).

Figure 2.4 represents the stress-strain model behavior the truss system to model the approximate response of the lap-spliced bars. In this model, the lap splice section reaches

the maximum peak strength $f_{s,max}$ until the surrounding concrete splits up. At this point, the section experiences a steep softening behavior due to splitting of surrounding concrete until it reaches the point of constant frictional stress $f_r$ developed across the failure interface. The corresponding strain values are $\varepsilon_s$ and $\varepsilon_r$, respectively.

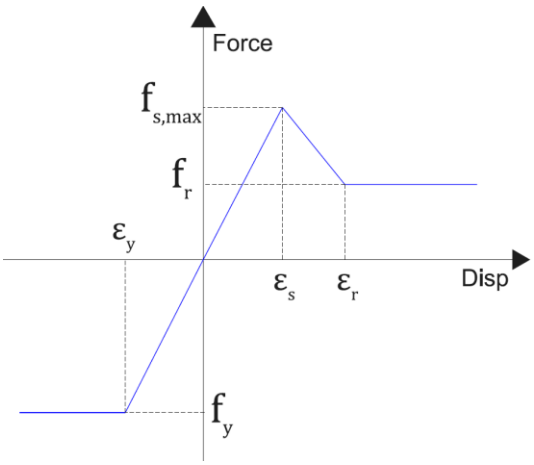


**Figure 2.4 – Stress-Strain Curve for Lap Splice Model**

The truss analogy assumes development of a uniform compressive field across the spliced bars at an angle approximately equal to 45°. The concrete surrounding the lap splice acts as compression struts to transfer the load between the bars. The mechanism considers the lap-splice failure by considering the formation of fracture surfaces perpendicular to the column surface to allow the relative movement between bars. Thus, with each longitudinal bar, an associated characteristic concrete block, as depicted in Figure 2.5, of length equal to the lap-splice length $l_s$ and perimeter $p$ is assumed to contribute to the splice strength.

The perimeter $p$ of the characteristic concrete block for rectangular and circular column cross-section can be calculated as follows:

$$p = \frac{s_l}{2} + 2(d_b + c) \leq 2\sqrt{2}\,(d_b + c) \tag{1}$$

where $s_l$ is the center-to-center spacing between the longitudinal bars, $d_b$ is the diameter of the longitudinal bars and c is the clear concrete cover. On the other hand, for a circular column cross-section, the perimeter of the characteristic block can be written as:

$$p = \frac{\pi D}{2n} + 2(d_b + c) \leq 2\sqrt{2}\,(d_b + c) \tag{2}$$

where $n$ is the number of evenly distributed longitudinal around the core of diameter $D$ of the column. MacKay (1989) concluded that the confined concrete did not add much to the lap-splice strength in the case cyclic loading, hence, the derivation ignores the strength contribution due the confined concrete to the lap-splice section.

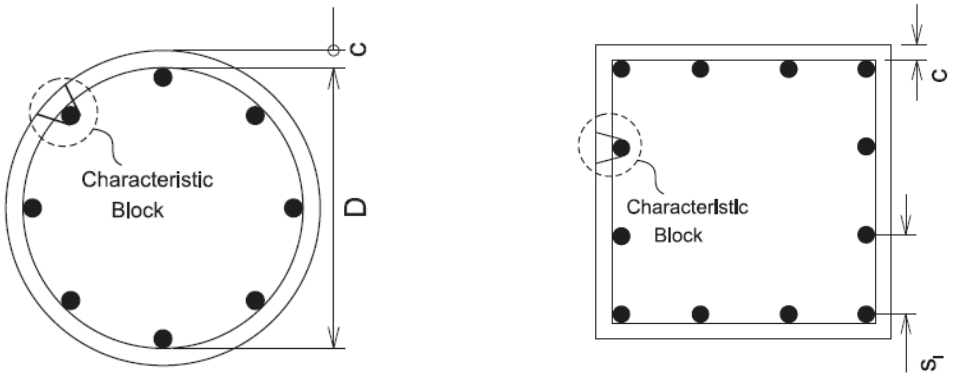


(a) (b)

**Figure 2.5 – Fictitious Characteristic Block for (a) Circular and (b) Square Column.**

Thus, satisfying the equilibrium of the free body diagram of the system, the maximum force $T_b$ in the longitudinal reinforcement bar can be expressed in terms of concrete tensile strength $f_t$ as follows:

$$T_b = A_b\, f_s = f_t\, p l_s \tag{3}$$

Once the lap-splice section reaches its maximum stress capacity $f_s$, the stress drops down to a constant value of residual stress $f_r$. The residual stress can be calculated by the shear-friction concept by estimating the shear force contribution by the transverse reinforcement crossing the cracked plane as follows:

$$\mu n_l n_t A_h f_h = n A_b f_r \tag{4}$$

where $n_l$ denotes the number of transverse reinforcement legs perpendicular to the cracked plane, $n_t$ the number of transverse reinforcement bars crossing the cracked plane, $A_h$ is the crack surface area, $f_h$ is the yield strength of the transverse reinforcement, $n$ is the number of longitudinal rebars in the tension side of the column.

The strain can be taken equal to the elastic yield strain of the bar, however, Tariverdilo (2009) assumed an additional slip displacement $u$ equal to 1 mm (= 0.0393'') at yield point that must be added to the elastic strain. This additional displacement is assumed to occur due to the bar slip over a fictitious length $l_{ss}$. It must be noted that this length is different lap splice length. Tariverdilo (2009) evaluated the impact of lap splice of risk estimated of reinforced concrete columns assuming that the slip occurs over a length equal to the depth of the column section. Thus, the total strain at the peak stress as be written as:

$$\varepsilon_s = \frac{f_y}{E_S} + \frac{u}{l_{ss}} \tag{5}$$

where $E_S$ is the elastic modulus of the rebar.

At residual stress $f_r$, the strain $\varepsilon_r$ is calculated by assuming a slip $u$ equal to 10 mm (= 0.3937 in.) that is approximately equal to the lug distance on the bar and can be written as:

$$\varepsilon_r = \frac{u}{l_{ss}} \tag{6}$$

## 2.4 Effects of variables on Splice Strength

It is observed from the equations discussed in Section 2.3 that the lap splice strength is a function of several variables such as lap splice length, column cross-section, reinforcement ratio, etc. Therefore, it is desirable to investigate the impact of these variables on the lap splice strength. The following subsections present a parametric study on the strength of the lap splice due to each of these variables. To isolate the effect of one variable, other variables are kept constant and equal to the most commonly used values in Georgia bridge columns.

### *2.4.1 Effect of Lap Splice Length*

An adequate lap splice length is required to transfer the force from one rebar to another in a spliced section. While most of the experimental tests on lap splice lengths show that it has an important role to play in the splice strength, Paulay (1982) stated that increasing length of a lap splice in columns in case of cyclic loading is of very little benefit because of the "unzipping" effect. Despite the plethora of research on the impact of lap splices, there is no clear agreement between the relation of the lap splice length and column

capacity. In this study, this relation is investigated purely through the theoretical point of view.

From Equation 3, it is observed that the maximum stress developed in the lap splice is directly proportional to its length from the theoretical point of view. In the present study, the effect of length of the spliced section is evaluated for the range of commonly used splice spacing in the state of Georgia. From the inventory analysis, it is discovered that the old highway bridge columns in Georgia used lap splices as short as 4.5''. However, the most commonly used lap splice lengths are 6.5'' and 9''. Figure 2.6 shows the stress-stress plot for these two lap splice lengths for a typical bridge column layout used in Georgia. This column has a height of 18' and cross-sectional dimensions 3' by 3'. The transverse reinforcement is equal to 12''.

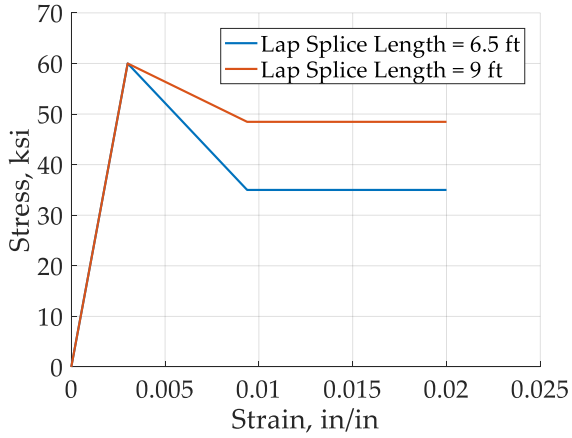


**Figure 2.6 – Lap Splice Stress-Strain Plot for Commonly Used Splice Lengths of 6.5 ft. and 9 ft. in Georgia.**

Figure 2.7 also shows the impact of the lap splice lengths ranging from 4' to 14' on the peak stress and residual stress of the lap splice of the same column. It is interesting to note that the peak stress is not affected by change in length of the spliced section. On the other hand, the residual stress shows a steep increase as the length of the lap splice

increases. For this column configuration, it is observed that the residual strength of the spliced section matches the peak strength at about the lap splice length of 11'.

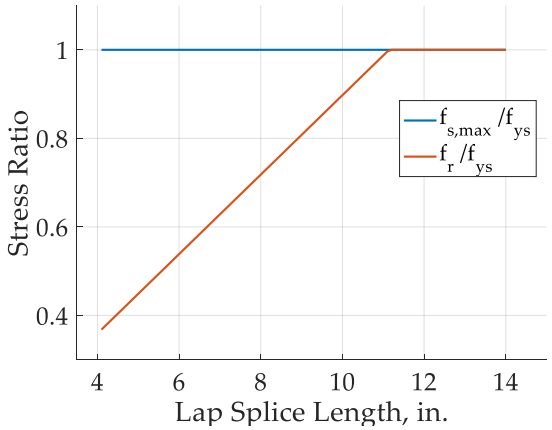


**Figure 2.7 – Effect of Change in Lap Splice Length on Peak and Residual Stress of Spliced Section.**

### *2.4.2 Effect of Transverse Reinforcement*

Hamad et al. (2002) have documented the effects of transverse reinforcement on spliced section through experimental tests. Their research revealed that presence of adequate transverse reinforcement helped to reduce splitting of cracks along the lap splice length, hence, improved the ductility of columns significantly. This is in agreement with the findings of many other researchers who performed experimental results to assess the effect of confinement on lap splices (Abdel-Kareem and Abousafa 2013; Mabrouk and Mounir 2017).

Adequate transverse reinforcement spacing not only helps to confine the core concrete in a structural member but also allows the lap splice section to develop enough shear friction after its strength goes past the peak strength. This effect depends on the type

(such as hoops, spiral, or ties) and shape (such as circular, square, or rectangular) of confining transverse reinforcement. To model the effect of confinement on concrete, a widely-accepted stress-strain model of concrete formulated by Mander et. al. (1988) has been used in this study. On the other hand, the effect of confinement on the post-peak lap splice strength is evaluated using Equation 4.

Before the introduction of AASHTO Seismic Design Specifications (2014) in the GDOT manual, the most commonly used reinforcement spacing for Georgia bridge columns was 12". However, the latest seismic design provisions suggest that the transverse spacing shall not exceed one-quarter of the minimum member dimension or 4.0 in. center-to-center. In the present study, the effect of transverse reinforcement spacing is studied for the lap splice length of 6.5'. The column reinforcement detailing for this case is same that was in Section 2.4.1.

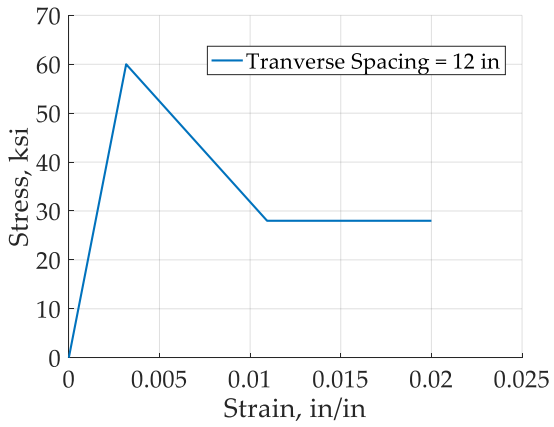


**Figure 2.8 – Lap Splice Stress-Strain Plot for Commonly Used Transverse Spacing of 12 in Georgia.**

Figure 2.9 depicts the effect of transverse spacing on the lap splice behavior. Same as the effect of the lap splice length, the peak strength is not affected by the change in transverse reinforcement spacing. On the other hand, there is the residual strength of the

lap splice drops considerably as the transverse reinforcement spacing is more than about 5.5'' for this cross-section.

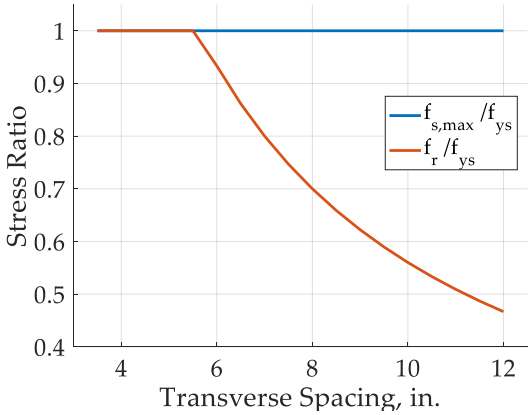


**Figure 2.9 – Effect of Change in Transverse Reinforcement Spacing on Peak and Residual Stress of Spliced Section.**

### *2.4.3 Effect of Steel Yield Strength*

According to Equation 4, the steel yield strength plays an important role in development of the bond between the steel rebars and surrounding concrete. The steel strength governs the level of forces that can be transferred through the steel-concrete interface in a spliced section. Moreover, the stress-strain curve of the steel reinforcement also governs the bond slip and strength characteristics which can lead to splitting and shear failures.

The commonly used longitudinal steel rebars in Georgia bridge columns have yield strengths of either 40 ksi and 60 ksi. Figure _ shows the variation of stress and strain for s

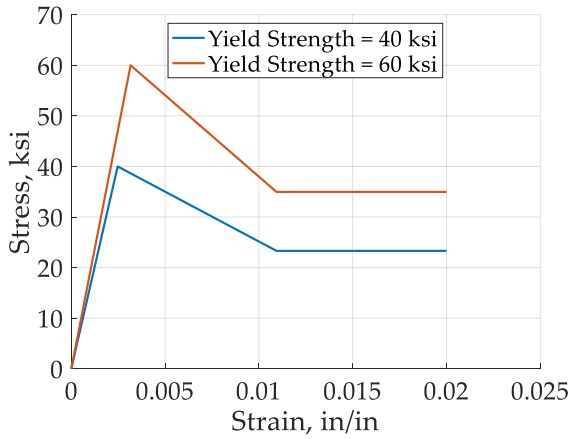


**Figure 2.10 – Lap Splice Stress-Strain Plot for Commonly Used Steels in Georgia.**

Figure 2.11 shows the effect of this parameter on the peak and residual stresses of the lap spliced section. The plot reveals that both parameters show a steep increase with the increase of steel strength.

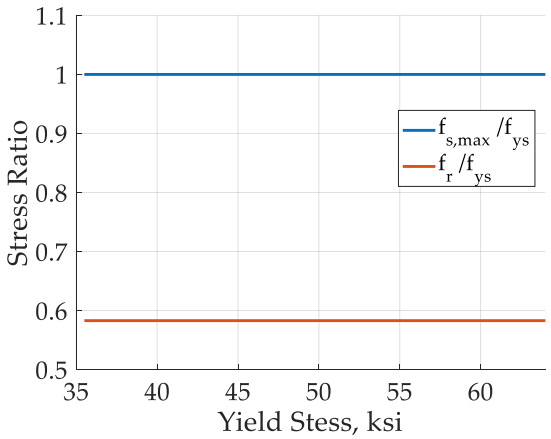


**Figure 2.11 – Effect of Change in Steel Yield Strength on Peak and Residual Stress of Spliced Section.**

### *2.4.4 Effect of Rebar Diameter*

In addition to the yield strength, the diameter of the reinforcement bars also affects the stress-strain curve of a spliced section. The ratio of cross-sectional to surface area of the rebar is directly proportional to the diameter of the rebar. This ratio is impacts the bond stress concentration of in the rebar.

The most commonly used rebar size for Georgia bridge is #11. Figure 2.12 shows the stress-strain curve for a typical Georgia column when 12 equally spaced #11 rebars are used as longitudinal reinforcement.

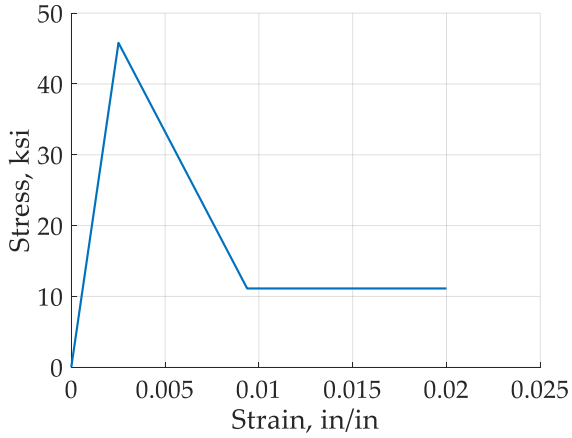


**Figure 2.12 – Lap Splice Stress-Strain Plot for Commonly Used #11 Rebar in Georgia.**

Additionally, Figure 2.13 shows the effect of the rebar diameter on the lap splice. As can be observed from the figure, larger diameters are not a good choice for spliced sections as there is a steep reduction in residual stress which could lead to ductility degradation of the structural member. The steep reduction in the post peak strength is due to larger bond stress concentrations resulting from greater cross-section area to surface area ratio for larger diameter rebars.

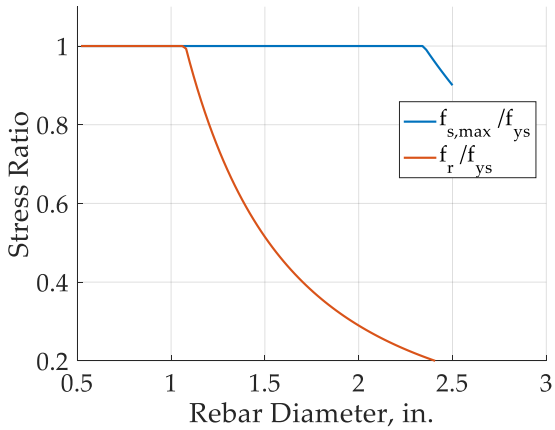


**Figure 2.13 – Effect of Change in Longitudinal Rebar Diameter on Peak and Residual Stress of Spliced Section.**

# CHAPTER 3. GEORGIA SEISMIC HAZARD MAPS AND BRIDGE INVENTORY ANALYSIS

In order to assess the impact of the LRFD Seismic Bridge Design Specifications in Georgia, it's important to determine the potential hazard associated with earthquakes in different parts of the state. Seismic Design Response Spectra and Seismic maps based on five site classes from A through E are developed in this chapter. Additionally, a thorough understanding of the bridge inventory is essential to determine the important bridge types to conduct the further analysis of the research. This chapter provides an analysis of the bridge inventory for the state of Georgia, based on the National Bridge Inspection (NBI) database and specific bridge plans provided by the Georgia Department of Transportation (GDOT).

## 3.1 Georgia Design Response Spectrum

Natural hazards can impose severe demands on any type of structures. U.S. Geological Survey reveals that at least 40% of the highway bridges can be expected to have a possibility of damage due to earthquakes during their service life. Hence, design codes and specifications are constantly revised and updated to incorporate any new information that is gained from experience, research, etc. Bridges should have considerable ductility and deformability to resist earthquake forces. With the idea of performance-based earthquake engineering (PBEE), the latest AASHTO LRFD Design Specifications (2014) recommend that bridges should be designed using displacement-based rather than force-based procedures. PBEE methodology aims at assuring that a desired level of structural

performance with definable levels of reliability is achieved when it is subjected to various levels of seismic input. The performance of the structure is measured in terms of Engineering demand parameters (EDPs) like curvature ductility, displacement, drift ratio, etc. In this study, such EDPs are employed to measure the damage of various components of the bridge.

Bridges that are in accordance with the LRFD provisions are expected to resist low to moderate seismic loads within the elastic range. In an event of high seismic loads, bridges are designed to suffer significant damages, however, they should have a low probability of collapse. Keeping this performance objective in consideration, seismic hazard is defined based on a 1000-year design return period earthquake which corresponds to 7% probability of exceedance in 75 years.

The AASHTO LRFD specification (2014) states that the seismic hazard at a location shall be characterized based on the acceleration spectrum of the location and relevant site factors. There are two procedures for determination of the acceleration spectrum given in the code: a) General Procedure, b) Site-Specific Procedure. The specification lists four conditions as to when the Site-Specific procedure shall be followed, however, because this study focusses on an overall study analysis of bridges across the state of Georgia, hence, the general procedure is followed.

The General Procedure uses the peak ground acceleration coefficient $PGA$, short-period spectral acceleration $S_S$, and long-period spectral acceleration $S_1$ to establish the design spectral acceleration curve. These coefficients can be obtained from the seismic design hazard maps developed by United States Geological Survey (USGS) for the 2007

AASHTO specifications. For the state of Georgia, the maps for obtaining the ground acceleration coefficient, short-period and long period accelerations are shown in Figure 3.1. It must be noted that these coefficients are only valid for rock site conditions (Site Class B) which is taken as the reference site class in the specification. Different site class adjustment factors are provided to account for the effects of other site classes. All these coefficients are in accordance with performance based on 1000-year return period and keep in consideration the performance based design objectives as stated earlier.

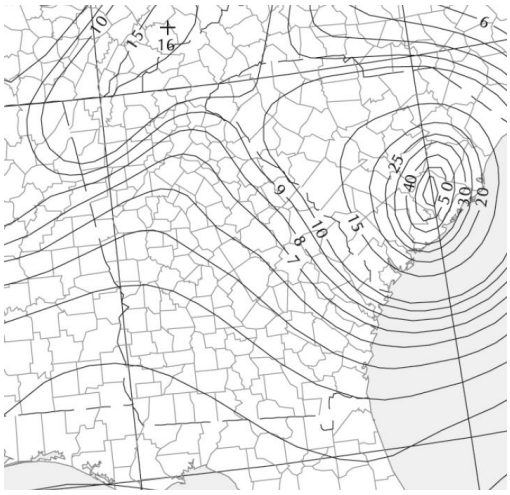


**Figure 3.1(a)**

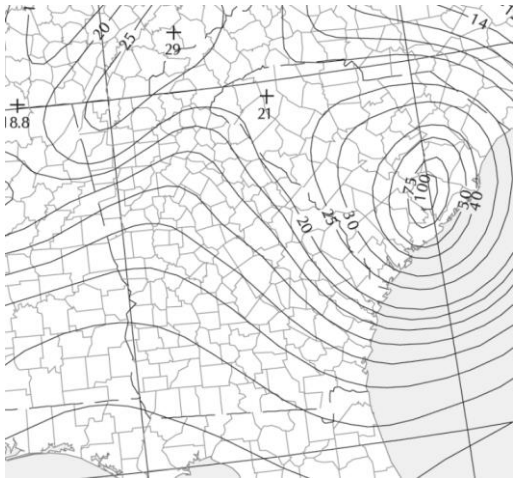


**Figure 3.1(b)**

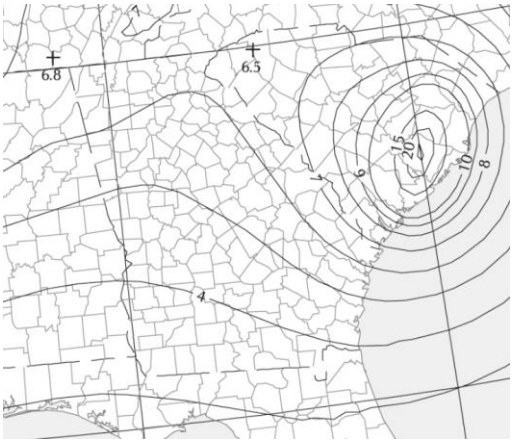


**Figure 3.1(c)**

**Figure 3.1 – Map of Georgia Depicting Contour Lines for Seismic Site Class B for (a) Horizontal Peak Ground Acceleration (PGA) Coefficient; (b) Horizontal**

**Response Spectral Acceleration Coefficient at Period 0.2 Seconds ($S_S$); and (c) Horizontal Response Spectral Acceleration Coefficient at Period 1.0 Second ($S_1$) (AASHTO, 2014).**

The type of surrounding soil can have a significant impact on the forces that are transmitted to a structure. To incorporate the site conditions, the specification classifies a site as A through F as per the site class definitions. These site class definitions are based on the type of soil and average shear wave for the upper 100 ft. of the soil profile. Site adjustment factors $F_{PGA}$ (for $PGA$) in Table 3-1, $F_a$ (for $S_S$) in Table 3-2 and $F_v$ (for $S_1$) in Table 3-3, are used to determine the site-specific acceleration spectrum coefficients $A_S$, $S_{DS}$ and $S_{D1}$, respectively. These coefficients are then used to plot the design spectral acceleration curve for a region as per Figure 3.2.

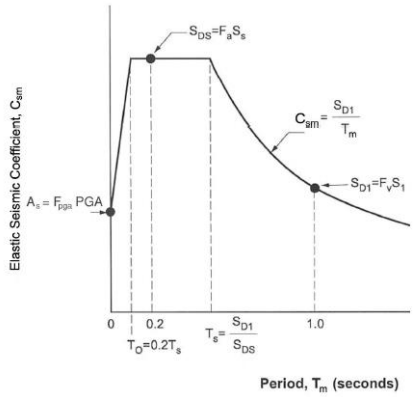


**Figure 3.2 – Design Response Spectrum (AASHTO, 2014)**

**Table 3-1 – Values of Site Factor, $F_{PGA}$, at Zero Period on Acceleration Spectrum (AASHTO, 2014).**

| Site Class | Peak Ground Acceleration Coefficient (PGA) | | | | |
|---|---|---|---|---|---|
| | PGA < 0.10 | PGA = 0.20 | PGA = 0.30 | PGA = 0.40 | PGA =0.50 |
| A | 0.8 | 0.8 | 0.8 | 0.8 | 0.8 |
| B | 1.0 | 1.0 | 1.0 | 1.0 | 1.0 |
| C | 1.2 | 1.2 | 1.1 | 1.0 | 1.0 |
| D | 1.6 | 1.4 | 1.2 | 1.1 | 1.0 |
| E | 2.5 | 1.7 | 1.2 | 0.9 | 0.9 |

**Table 3-2 – Values of Site Factor, $F_a$, for Short Period Range of Acceleration Spectrum (AASHTO, 2014).**

| Site Class | Spectral Acceleration Coefficient at Period 0.2 second | | | | |
|---|---|---|---|---|---|
| | $S_S < 0.25$ | $S_S = 0.50$ | $S_S = 0.75$ | $S_S = 1.00$ | $S_S > 1.25$ |
| A | 0.8 | 0.8 | 0.8 | 0.8 | 0.8 |
| B | 1.0 | 1.0 | 1.0 | 1.0 | 1.0 |
| C | 1.2 | 1.2 | 1.1 | 1.0 | 1.0 |
| D | 1.6 | 1.4 | 1.2 | 1.1 | 1.0 |
| E | 2.5 | 1.7 | 1.2 | 0.9 | 0.9 |

**Table 3-3 – Values of Site Factor, $F_v$, for Long Period Range of Acceleration Spectrum (AASHTO, 2014).**

| Site Class | Spectral Acceleration Coefficient at Period 1.0 second | | | | |
|---|---|---|---|---|---|
| | $S_1 < 0.10$ | $S_1 = 0.20$ | $S_1 = 0.30$ | $S_1 = 0.40$ | $S_1 > 0.50$ |
| A | 0.8 | 0.8 | 0.8 | 0.8 | 0.8 |
| B | 1.0 | 1.0 | 1.0 | 1.0 | 1.0 |
| C | 1.7 | 1.6 | 1.5 | 1.4 | 1.3 |
| D | 2.4 | 2.0 | 1.8 | 1.6 | 1.5 |
| E | 3.5 | 3.2 | 2.8 | 2.4 | 2.4 |

In the present study, Site Classes A to E are studied and the design response spectra for these site classes, as obtained by utilizing the above-mentioned coefficients, are shown in Figure 3.3. All the site classes but Site Class F are considered because of unavailability of soil properties data for Georgia. The reason for exclusion of Site Class F is that it requires site-specific investigations to determine the influence of the local site conditions on the structure. Thus, it requires the site-specific procedure to determine the design acceleration response spectrum.

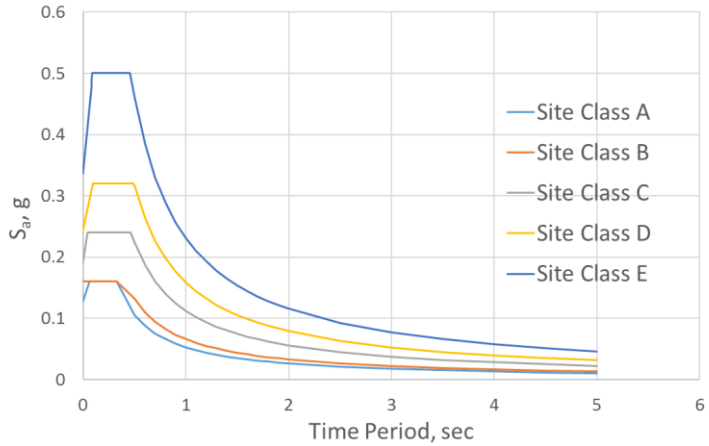


**Figure 3.3 – Georgia Design Response Spectra for Site Classes A, B, C, D and E.**

To estimate the seismic vulnerability of highway bridges in Georgia, an appropriate suite of ground motions is essential. Due to unavailability of ground motion records, past researchers have used artificially generated ground motions to study Central and South-eastern United States (CSUS). Nielson (2005) used Rix and Fernandez (Rix and Fernandez-Leon, 2004) ground motion suites to determine seismic vulnerability of highway bridges in Central and South-eastern United States (CSUS). Because Georgia falls under CSUS region, a suite of 48 Rix and Fernandez ground motions are used to assess the seismic

vulnerability of bridges in this study. Figure 3.4 shows a plot of the spectral acceleration values for a range of structural time periods obtained from these 48 ground motions.

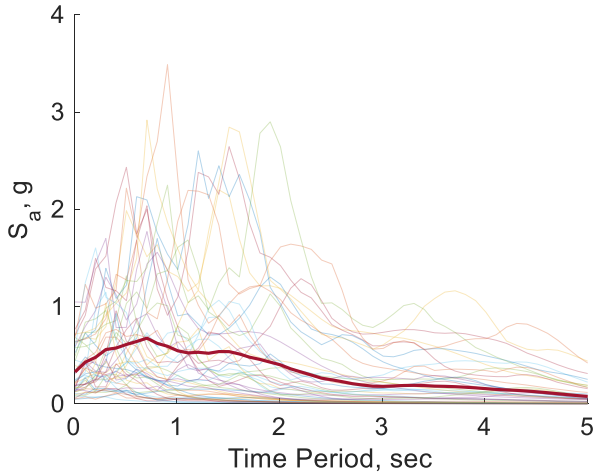


**Figure 3.4 – Spectral Acceleration Plot for a Range of Time Periods for the 48 Rix and Fernandez Ground Motion Suite.**

### *3.1.1 Seismic Zones*

As performance is the main criteria to be followed while designing a bridge using PBEE methodology, the code suggests to classify the region under study into seismic zones. While designing a bridge for earthquake effects, these zones help the designer to determine the type of analysis, detailing requirements, etc. to be used for the bridge. The greater the zone number, the more rigorous should the design be. Table 3-4 shows the boundaries that are used to define these zones; these boundaries are based on the design spectral acceleration coefficient at 1-second, $S_{D1}$. Although the LRFD code specifies only 4 zones, Zone 1 is subdivided into two subzones, Zone 1-A and 1-B, for the sake of this study based on the recommendations by GDOT.

**Table 3-4 – Seismic Zone Boundaries.**

| Seismic Zone | Acceleration Coefficient Range |
|---|---|
| 1-A | $S_{D1} < 0.10$ |
| 1-B | $0.10 < S_{D1} < 0.15$ |
| 2 | $0.15 < S_{D1} < 0.30$ |
| 3 | $0.30 < S_{D1} < 0.50$ |
| 4 | $S_{D1} > 0.50$ |

It must be noted that these zone definitions are based on $S_{D1}$, hence they incorporate the local seismic and site effects. Therefore, a site on a rock site conditions might fall under a different seismic zone than a nearby site that has soft soil conditions. This concept is elaborated in the next section which presents the seismic zone maps for all the site classes for Georgia.

## 3.2 Georgia Site-Specific Seismic Hazard Maps

Seismic hazard maps are helpful to determine the predicted level of ground motion excitation for a region in consideration. In the present study, the state of Georgia is divided into 6 regions, as shown in Figure 2.4, based on the expected maximum peak ground acceleration (PGA) intensity. The northern region of the state is most susceptible to higher intensity earthquakes because of its proximity to South Carolina which has a rich history of seismic activity.

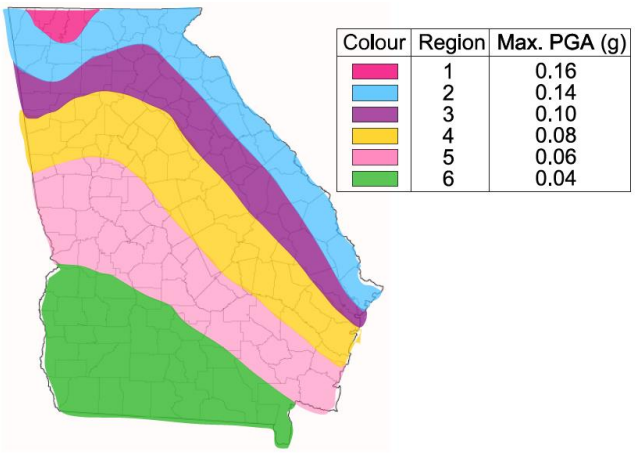


**Figure 3.5 – The Map of Georgia Showing Six Zones Considered in the Study.**

### *3.2.1 Site Class A Seismic Hazard Map*

Site Class A is characterized by very hard rock site conditions where the average shear seismic wave velocity is greater than 5,000 ft./sec. The seismic hazard map for this site class for Georgia is shown in Figure 3.6. The maximum earthquake intensity level for Site Class A is 0.13 g. Hard rocky sites result in large attenuation distances and allow earthquake waves to spread over a vast region depending on the its intensity, however, the seismic intensity is the lowest compared to the other site classes. Because of the low seismic hazard level, the whole state falls under seismic zone 1-A.

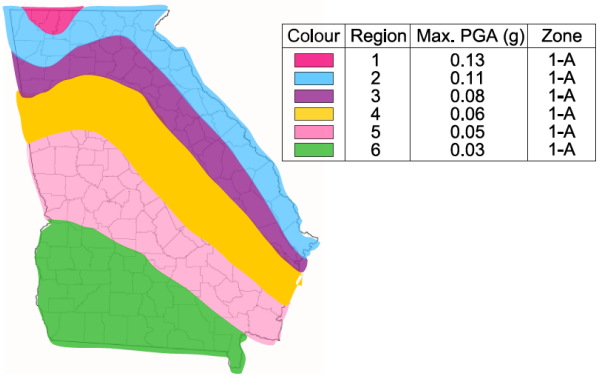


**Figure 3.6 – Georgia Seismic Hazard Map for Site Class A**

### *3.2.2 Site Class B Seismic Hazard Map*

Site Class B is characterized by relatively softer rock site conditions than Site Class A with an average seismic wave velocity between 2,500 and 5,000 ft./sec. As Shown in Figure 3.7, the whole state falls under Seismic Zone 1-A and doesn't require consideration of rigorous seismic structural analysis for design. The maximum PGA for Site Class B is 0.16 g.

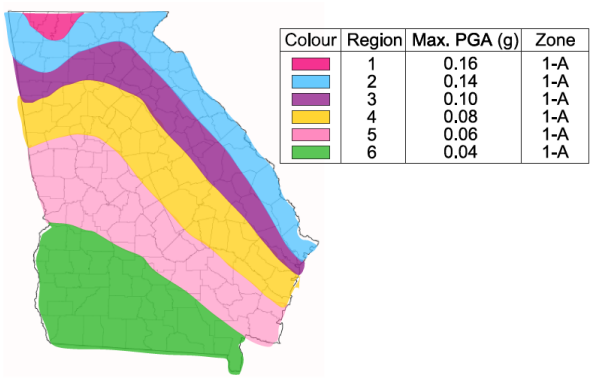


**Figure 3.7 – Georgia Seismic Hazard Map for Site Class B**

### *3.2.3 Site Class C Seismic Hazard Map*

Site Class C is characterized by very dense soil or rock where the average shear wave velocity ranges from 600 to 1200 ft./sec. The maximum PGA range for different regions for this site class is 0.05g to 0.19g. As depicted in Figure 3.8, Regions 1 and 2 fall in Seismic Zone 1-B for Site Class C, whereas the rest of the state still falls in Seismic Zone 1-A.

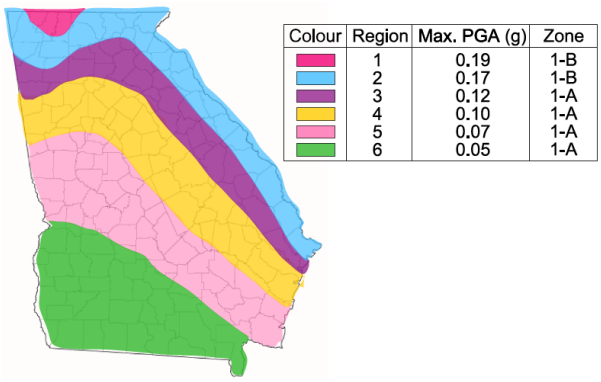

| Colour | Region | Max. PGA (g) | Zone |
|---|---|---|---|
| | 1 | 0.19 | 1-B |
| | 2 | 0.17 | 1-B |
| | 3 | 0.12 | 1-A |
| | 4 | 0.10 | 1-A |
| | 5 | 0.07 | 1-A |
| | 6 | 0.05 | 1-A |

**Figure 3.8 – Georgia Seismic Hazard Map for Site Class C**

### *3.2.4 Site Class D Seismic Hazard Map*

Site Class D has softer site class conditions compared to Site Class C leading to amplification of seismic waves and is characterized by average shear velocity less than 600 ft./sec. Figure 3.9 shows the seismic hazard map for Georgia for Site Class D. The Seismic Zone intensity increases from south to north of the state with maximum PGA equal to 0.24 g.

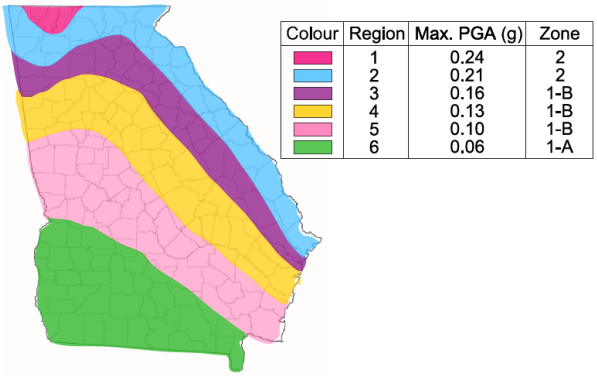

| Colour | Region | Max. PGA (g) | Zone |
|---|---|---|---|
| | 1 | 0.24 | 2 |
| | 2 | 0.21 | 2 |
| | 3 | 0.16 | 1-B |
| | 4 | 0.13 | 1-B |
| | 5 | 0.10 | 1-B |
| | 6 | 0.06 | 1-A |

**Figure 3.9 – Georgia Seismic Hazard Map for Site Class D**

### *3.2.5 Site Class E Seismic Hazard Map*

Site Class E site conditions are known to be highly reactive to seismic ground motions. The soil composition at these sites mainly consists of clayey or other type of soft soils. Such soils are very susceptible to high moisture changes which allow amplification of the ground motion. The seismic hazard map for Georgia for Site Class E is shown in Figure 3.10. Most of the state falls under Seismic Zone 2 for this site class with the maximum PGA being 0.35 g in Region 1.

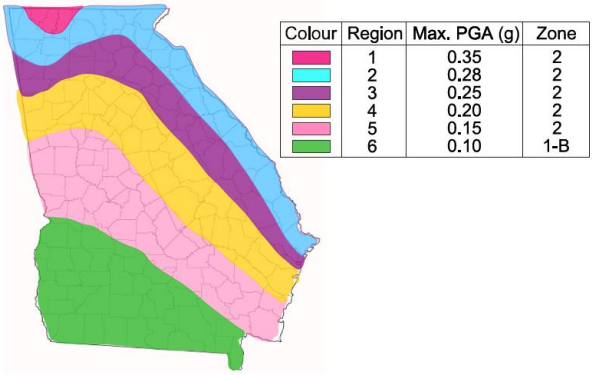


**Figure 3.10 – Georgia Seismic Hazard Map for Site Class E**

## 3.3 Georgia Highway Bridge Inventory Analysis

The ideal way to assess the vulnerability of bridges would be to model each bridge and obtain the fragility curve of the bridge. However, due to complexity of this approach, it is recommended to group bridges into various classes. Nielson (2005) used this approach to classify bridges based on the type of construction and materials used in the bridges. The present study also makes use of such a classification. It's assumed that bridges falling in a bridge class behave in a similar way during an earthquake event. Therefore, fragility curves are generated for bridges classes rather than individual bridges.

The National Bridge Inventory (NBI) database, maintained by Federal Highway Association (FHWA), records the information about all the highway structures for every state in the US. The NBI database provides basic information of 15,122 highway structures in Georgia. Many of those structures are tunnels and culverts, which are assumed to represent a different type of system and therefore, not considered in this study. For the remaining 9,514 bridges, a preliminary statistical distribution analysis using two key NBI fields (material and construction type) was performed to determine a more general classification of the inventory. Although detailed bridge characteristics must be studied from the individual bridge plans, the database provides important characteristics such as material type, dimensions, number of spans, skew angle, structural rating, etc.

Table 3-5 shows the distribution of bridges in Georgia based on the construction material type listed in NBI database (FHWA, 2002). The construction material used in Georgia is predominantly concrete, followed by steel. Similarly, Table 3-6 shows the distribution of bridges in Georgia based on construction types listed in NBI (FHWA, 2002).

**Table 3-5 – Georgia Highway Bridges Classified as per Their Construction Material (FHWA, 2002).**

| Construction Materials | Number of Bridges | Percentage |
|---|---|---|
| Concrete | 3,227 | 33.9 |
| Concrete Continuous | 124 | 1.3 |
| Steel | 2,501 | 26.3 |
| Steel Continuous | 1,101 | 11.6 |
| Prestressed Concrete | 2,321 | 24.4 |
| Prestressed Concrete Continuous | 116 | 1.2 |
| Wood or Timber | 118 | 1.2 |
| Masonry | 3 | 0.0 |
| Aluminium, Wrought Iron, or Cast Iron | 1 | 0.0 |
| Other | 2 | 0.0 |

**Table 3-6 – Georgia Highway Bridges Classified as per Their Construction Type (FHWA 2002).**

| Construction Type | Number of Bridges | Percentage |
|---|---|---|
| Slab | 1,135 | 11.9 |
| Stringer/Multi-beam or Girder | 5,646 | 59.3 |
| Girder and Floor Beam System | 63 | 0.7 |
| Tee Beam | 2,123 | 22.3 |
| Box Beam or Girders – Multiple | 230 | 2.4 |
| Box Beam or Girders – Single or Spread | 131 | 1.4 |
| Frame (Culverts Excluded) | 24 | 0.3 |
| Truss – Thru | 51 | 0.5 |
| Arch – Deck | 55 | 0.6 |
| Others | 95 | 0.6 |

After careful examination of the NBI database, all the bridges in Georgia are assigned one of seven bridge classes based as given in Table 3-7. It is assumed that the bridges grouped in these classes would have similar responses to seismic excitation. Multi-span simply supported concrete bridge class is the most common bridge class in Georgia and represents about 41.03% bridges in the state. As this study focusses on impact of seismic transverse spacing and lap splices in bridge columns, only multi-span bridges have been considered hereafter.

**Table 3-7 – Georgia Bridge Classes and Their Proportions (FHWA 2002).**

| Bridge Class | Abbreviation | Number | Percentage |
|---|---|---|---|
| Multi-Span Continuous Steel Girder | MSC Steel | 1,065 | 11.9 |
| Multi-Span Simply Supported Concrete Girder | MSSS Concrete | 3,904 | 41.03 |
| Multi-Span Simply Supported Steel Girder | MSSS Steel | 1,516 | 15.93 |
| Multi-Span Simply Supported Slab | MSSS Slab | 951 | 10.00 |
| Single-Span Concrete Girder | SS Concrete | 362 | 3.80 |
| Single-Span Steel Girder | SS Steel | 721 | 7.58 |
| Other | Other | 995 | 10.46 |

### *3.3.1 Bridge Class Statistics*

With the bridge classes defined, an examination of key bridge characteristics is necessary to select a representative bridge from each bridge class. Although the NBI database provides the basic bridge characteristics for bridges, detailed information of the representative bridge from each bridge class is obtained by carefully studying the bridge plans. This step is necessary to generate accurate finite element models of bridges. The following characteristics, obtained from the NBI database, provide an insight into typical geometric configuration of bridges in each bridge class:

- Number of spans (presented in Table 3-8)
- Maximum span length (presented in Table 3-9)
- Deck width (presented in Table 3-10)
- Minimum vertical clearance (presented in Table 3-11)

The mode for most of the bridge classes in Georgia is 3. Hence, to be compare the results across the bridge classes, all the bridge classes in this study consider only 3 span bridges for each bridge class. Other parameters are chosen as close as close to the median values of the bridge class depending on the availability of bridge plans.

**Table 3-8 – Span Number Statistics for Four Bridge Classes Considered.**

| Bridge Class | Mean | Standard Deviation | Median | Maximum | Minimum | Mode |
|---|---|---|---|---|---|---|
| MSC Steel | 4.57 | 3.72 | 4 | 41 | 2 | 4 |
| MSSS Concrete | 5.17 | 4.49 | 4 | 89 | 2 | 3 |
| MSSS Steel | 3.97 | 2.27 | 3 | 40 | 2 | 3 |
| MSSS Slab | 5.95 | 4.16 | 5 | 56 | 2 | 3 |

**Table 3-9 – Maximum Span Length Statistics for Four Bridge Classes.**

| Bridge Class | Mean | Standard Deviation | Median | Maximum | Minimum | Mode |
|---|---|---|---|---|---|---|
| MSC Steel | 82.22 | 45.87 | 83 | 280 | 10 | 27 |
| MSSS Concrete | 56.16 | 30.98 | 40 | 187 | 12 | 40 |
| MSSS Steel | 56.68 | 28.64 | 55 | 252 | 9 | 16 |
| MSSS Slab | 20.56 | 5.22 | 20 | 88 | 12 | 20 |

**Table 3-10 – Deck Width Statistics for Four Bridge Classes.**

| Bridge Class | Mean | Standard Deviation | Median | Maximum | Minimum | Mode |
|---|---|---|---|---|---|---|
| MSC Steel | 48.96 | 31.50 | 34.70 | 221.20 | 10.60 | 34.00 |
| MSSS Concrete | 47.18 | 25.47 | 41.30 | 522.40 | 12.40 | 41.30 |
| MSSS Steel | 47.28 | 33.89 | 34.30 | 220.10 | 8.00 | 25.20 |
| MSSS Slab | 28.12 | 6.69 | 25.80 | 96.00 | 12.00 | 25.20 |

**Table 3-11 – Minimum Vertical Deck Width Statistics for Four Bridge Classes.**

| Bridge Class | Mean | Standard Deviation | Median | Maximum | Minimum | Mode |
|---|---|---|---|---|---|---|
| MSC Steel | 17.62 | 3.10 | 16.11 | 42.09 | 10.06 | 16.07 |
| MSSS Concrete | 20.48 | 5.27 | 19.06 | 75.01 | 0.99 | 16.07 |
| MSSS Steel | 18.95 | 3.70 | 17.06 | 43.10 | 10.08 | 16.05 |
| MSSS Slab | 17.46 | 3.90 | 18.07 | 23.02 | 10.05 | 16.05 |

# CHAPTER 4. OVERVIEW OF FRAGILITY CURVES

In recent decades, fragility curves have become an important statistical tool to quantify the potential damage in a structure due to hazards. The first section of this chapter presents the general formulation used in this study to develop the fragility curves.

## 4.1 Analytical Fragility Curve Formulation

A fragility function $F$ represents the probability of the demand meeting or exceeding a predefined capacity damage state given the intensity measure of the hazard. Mathematically, the fragility function can be expressed as in terms of conditional probability as:

$$F = P[D - C \geq 0 | IM = y] \tag{7}$$

where $D$ is the demand of the structural component, $C$ is the capacity of the component, $IM$ is the intensity measure of the hazard and $y$ is the realization of the hazard intensity. If fragility functions are calculated and plotted over a range of realizations of the chosen intensity measure, it yields a fragility curve. Figure 4.1 shows one such fragility curve obtained for a specified limit state. On the x axis, this curve represents the considered intensity measure and on the y axis, it shows the associated risk. The intensity measure used to evaluate the fragility function in this study is peak ground acceleration (PGA).

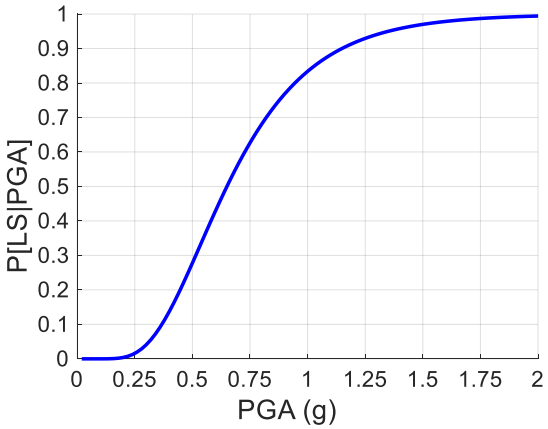


**Figure 4.1 – Typical Fragility Curve**

In the past, researchers have mostly used the following three methods to formulate fragility curves: a) expert-based, b) empirical, and c) analytical fragility curves. These methods could be combined with one another to obtain more accurate fragility estimation. In fact, a multi-hazard risk analysis tool distributed by Federal Emergency Management Agency (FEMA) called HAZUS-MH uses this kind of a hybrid approach to determine hazard risk analysis of structures (FEMA 2003). Another way of obtaining more robust fragility functions is to use advanced statistical techniques like Bayesian updating to combine analytical results obtained from computer simulations and field inspection results. With advancement in structural health monitoring, such hybrid techniques are generally preferred for research purposes.

Expert-based fragility curves were used to estimate the expected behavior of highway bridges in California due to data shortage (Rojahn and Sharpe, 1985). This method is not a popular method of quantifying the fragility functions anymore as there is a high level of uncertainty involved due to subjectivity of the procedure.

Empirical fragility curves rely on the post-hazard assessment of the structure to simulate the demand model. Many researchers used this methodology to formulate fragility functions after Loma Prieto and Northridge earthquakes (Basoz and Kiremidjian, 1999; Kiureghian, 2002; Shinozuka et. al., 2003). This method relies on evaluating fragility functions through collection of binary pass-fail data from experts for the failure of a structure after the hazard. One could argue that this method should be the most favored method of estimating damage risk because the damage risk is derived from the observations of the performance of the structure in real life. However, the major drawback of this method is that it requires an adequate number of structures from a bridge class to quantify the fragility functions. In practice, this data is limited. Moreover, as with the expert based method, there could be a high level of subjectivity in the post-hazard inspection data as well.

With improvement in technology in the past couple of decades, analytical fragility curves have been the most popular way to formulate the fragility functions. When enough bridge inspection or ground motion data is not available, computer simulations are used to quantify the capacity and/or demand of the structure in consideration. Usually the capacity of the structural component is determined based on experimental tests or its geometric interpretation, whereas the demand imposed on the component during a hazard is computed through computer simulations. Building an accurate finite element model of the structure and selecting appropriate ground motions are some of the important steps involved in this method.

### *4.1.1 Component-Level Fragility Curves*

Analytical fragility approach is used to estimate the fragility functions for components. Due to various kinds of variabilities involved such as geometric, hazard, etc., the capacity and demand models are random variables, rather than deterministic numbers. If both component capacity and demand models are assumed to follow a lognormal distribution, by the application of the central limit theorem, Equation 7 can be expressed as a lognormal cumulative distribution function in terms of the parameters of the capacity and demand variables as follows:

$$F = \Phi\left(\frac{\ln S_d/S_c}{\sqrt{\beta_d^2 + \beta_c^2}}\right) \tag{8}$$

where $S_d$ is the median parameter of the damage random variable, $\beta_d$ is the lognormal standard deviation of the damage random variable, $S_c$ is the median parameter of the capacity random variable and $\beta_c$ is the lognormal standard deviation of the capacity random variable. All these parameters are defined at each intensity level for which damage fragility is to be determined. From Equation 8, it is observed that the parameters of the capacity and demand random variable are needed to estimate the fragility function. The techniques used to define these parameters in the function are described in following sections.

### *4.1.2 System-Level Fragility Curves*

Component level fragility curves can be helpful to determine the most vulnerable links in the overall system. They can also be used to determine appropriate retrofit

strategies and component life-cycle cost analysis; however, these curves do not provide any information about the vulnerability of the complete structure. One component could be more susceptible to a ground motion than the other when a complete structure is analyzed. To assess the vulnerability of the structure, the component level curves must be combined to derive the system level fragility curves. Under the assumption that the system behaves as a series system, wherein the failure of one component results in the failure of the whole system, these curves can be combined to determine the system-level vulnerability. This assumption has been used by many researchers in the past (Nielson, 2005; Ghosh, 2013). Either closed form solution or numerical solution can be used to find the system fragility function depending on the number of components, complexity of the failure domains.

In this study, a numerical approach called Monte Carlo simulations is used to combine the component level fragility curves. This process involves generating $N$ random samples from both capacity and demand variable distributions. While generating the samples from the capacity side samples, the correlation between the limit states is assumed to be equal to 1 to ensure that the numerical samples from each limit states rank in the same order as the limit states are defined. On the other hand, while generating the samples from the demand side, correlations between the bridge components must be incorporated into sampling. After generating the samples, each sample from the demand and capacity side are paired with each other. The paired samples are compared one-to-one to evaluate the failure. If the sample from the limit state side is lesser than the sample from the demand side, the system is considered to have failed. Following this definition of failure, an indicator function is defined to track the number of failed sampled as follows:

$$I_f = \begin{cases} 1 & \text{if } (x_i, x_j) \in F_{ij} \\ 0 & \text{if } (x_i, x_j) \notin F_{ij} \end{cases} \quad (9)$$

where $x_i$ and $x_j$ are the realization of the i[th] and j[th] distributions and $F_{ij}$ is defined by the i[th] and j[th] limit state.

The indicator function can now be evaluated at equal intervals of a reasonable range of the intensity measure. At each value of the intensity measure, the failure probability can be estimated as:

$$P[LS|IM = y] = \frac{\sum_{i=1}^{N} I_{F_i}}{N} \quad (10)$$

It's important to determine a reasonable number of samples to obtain an accurate probability of failure. The results from the sensitivity analysis of the variation of the failure probabilities plotted with respect to number of samples. It is observed that approximately 150,000 samples are enough to stabilize the probability estimates.

### 4.2 Limit States

As stated in Section 4.1.1, limit state definitions are required to evaluate the fragility functions. In this study, the limit states of each component are based on either past experimental results or functional interpretation of the component. Engineering demand parameters (EDPs) such as displacement, curvature ductility, drift ratio, etc., have been used by researchers to define the limit states of columns. This is in accordance with the performance based seismic design philosophy in the latest AASHTO Design Specifications

(2014). These limit states are defined for 4 damage state levels: a) slight, b) moderate, c) extensive, and d) complete. Table 4-1 describes the definitions adopted for each limit state from HAZUS-MH (FEMA 2003). Each limit state is assumed to follow a lognormal distribution with the parameters of the distribution obtained from experimental data or past research.

**Table 4-1 – HAZUS' Qualitative Limit States (FEMA, 2003).**

| Limit State | Description |
|---|---|
| Slight | Hairline cracking in columns, minor spalling at column faces, minor cracking in plastic hinge regions. |
| Moderate | Shear cracks in columns, formation of plastic hinges or buckling of longitudinal rebars indicating flexural failure, cracks exposing column core, pile cap damage. |
| Extensive | Shear failure of columns, flexural failure due to inadequate confinement, anchorage or lap splice, vertical pull of longitudinal reinforcement, ground displacement at column base. |
| Complete | Column collapse, vertical or lap splice failure. |

The following subsections provide the descriptions of these limit states for each bridge component considered in the study. Although in the real-life situation the limit states are expected to vary with the service life of a structure due to aging, corrosion deterioration, etc., such factors are not considered in this study. Therefore, the limit states are assumed to be constant throughout the service life of the bridge.

### *4.2.1 Columns*

Static pushover tests on columns can be used to determine the force-deflection curves and column damage in terms of EDPs. Since the curvature of a structural member is a property of a cross-section and is independent of the length of the member, the chosen EDP for this study is curvature ductility. The curvature ductility $\mu_{\emptyset}$ of a structural member is defined as:

$$\mu_{\emptyset} = \frac{\kappa_{max}}{\kappa_{yield}} \tag{11}$$

where $\kappa_{max}$ is the maximum curvature observed in the column under seismic shaking, and $\kappa_{yield}$ is the column yield curvature.

In the present study, the following three cases corresponding to non-seismic and spacing lap splice and transverse reinforcement requirements are considered:

1. No Lap Splice with Non-Seismic Detailing: In this case, the lap splice is not provided at the base of the column and a non-seismic transverse reinforcement spacing of 12 in. is used.
2. Lap Splice with Non-Seismic Detailing: In this case, the lap splice is provided at the base of the column with transverse reinforcement spacing equal 12 in.
3. Lap Splice with Seismic Detailing: In this case, the lap splice is provided at the base of the column with transverse reinforcement spacing equal to 3 in.

The moment-curvature ductility plots along with the corresponding column limit states for the above-mentioned three cases are shown in Figure 4.2. The column capacities

in terms curvature ductility are adopted from previous experimental test results (ChaiI et. al., 1991; Sun et. al., 1993; Lehman, 2000; Calderone, 2001; Melek and Wallace, 2004; Freytag, 2006) that characterize four different damage state levels: Slight, Moderate, Extensive, and Complete damage states. The slight damage state corresponds to the curvature ductility at the first point of yield in the longitudinal rebar. The moderate damage state corresponds to the spalling of cover concrete due to expansive force. The extensive limit state corresponds to the exposure of concrete core or yielding of transverse reinforcement, whichever happens first. The complete damage state corresponds to the lap splice failure in the case of the lap splice column, or otherwise, longitudinal rebar buckling in the no lap splice case.

For the three cases of column seismic design considered in this study, the column limit states are presented in Table 4-2. It is assumed that the reduction of transverse reinforcement does not affect the column capacity as much, hence, for the seismic and non-seismic cases, the same limit state values have been assumed.

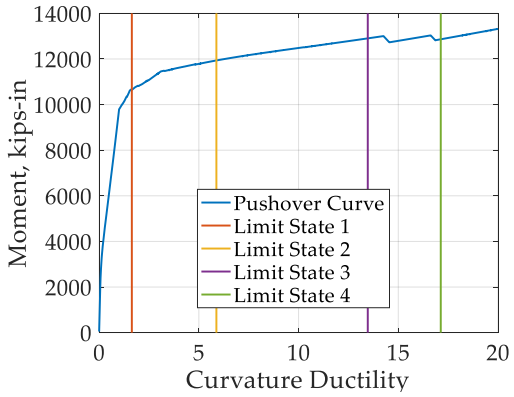


**Figure 4.2 (a)**

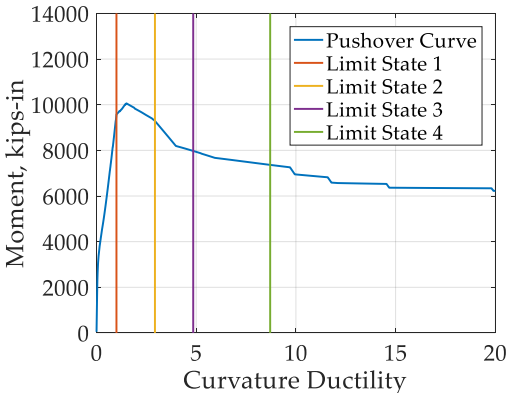


**Figure 4.2 (b)**

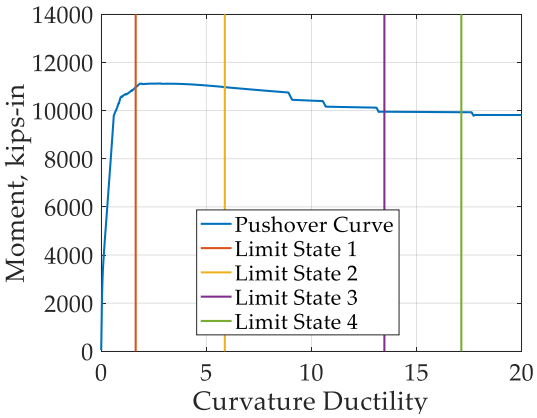


**Figure 4.2 (c)**

**Figure 4.2 – Moment-Curvature Ductility Curves and Limit States for: (a) Column with No Lap Splice and Non-Seismic Transverse Detailing; (b) Column with Lap Splice and Non-Seismic Transverse Detailing; and (c) Column with Lap Splice and Seismic Transverse Detailing.**

**Table 4-2 – Limit State Median Values for Lap Spliced Column Sections.**

| Case | Description | Slight | Moderate | Extensive | Complete |
|---|---|---|---|---|---|
| 1 | No Lap Splice & Non-Seismic Detailing | 1.64 | 5.88 | 13.47 | 17.13 |
| 2 | Lap Splice & Non-Seismic Detailing | 1.00 | 2.93 | 4.85 | 8.71 |
| 3 | Lap Splice & Seismic Detailing | 1.64 | 5.88 | 13.47 | 17.13 |

## 4.3 Probabilistic Seismic Demand Model

In addition to limit states, demand estimates are required to quantify the fragility functions of components. Probabilistic Seismic Demand Models (PSDMs) obtained from analytical seismic analyses of the structure are used for this purpose. PSDMs evaluate the peak structural demand of a component as a function of intensity of ground motions. In this study, the PSDM model is obtained from nonlinear time history analyses by running a suite of 48 ground motions to consider the uncertainty in the structural response. The data points for the peak demands of the components obtained from nonlinear time history and plotted against the value of peak ground accelerations (PGA) of that ground motion.

Cornell et al. (2002) suggested a power function model relation to estimate the median demand from PSDM using the following relation:

$$EDP = a\, IM^{b} \tag{12}$$

where a and b are, the coefficients obtained from the linear regression analysis of the model. To calculate these coefficients the demand model is transformed into the linear space by taking logarithm of both sides of Equation 12 to obtain the following equation:

$$\ln(EDP) = \ln(a) + b * ln(IM) \tag{13}$$

As stated before, the demand variable is assumed to follow a lognormal distribution in the study, hence, it follows a normal distribution in the linear space, with a mean equal to zero and a constant stand deviation $\sigma$.

# CHAPTER 5. MODELING AND DETERMINISTIC SEISMIC BRIDGE ANALYSES

This chapter presents bridge characteristics and modeling details that are employed to generate three-dimensional finite element models of the representative bridge from each multi-span bridge class in Georgia considered in this study. These 3-D models are useful to evaluate the expected seismic performance of bridges. The lap splice model, as explained in Chapter _, is incorporated into the analytical bridge models to estimate to compare their expected seismic performance for different detailing cases. Column and bearing responses from deterministic bridge analyses performed using a single ground motion are studies to assess the performance degradation due to inadequate lap splice lengths and confining reinforcement. As described in CHAPTER 4, the analytical fragility curve methodology requires the demand parameters to be obtained from these analytical bridge models. The chapter further explains the seismic response of various bridge components obtained from a deterministic nonlinear time history analysis.

## 5.1 Typical Highway Bridge Components

The typical bridge model used in this study was identified by Nielson (2005) who used conducted research on fragility functions for highway bridge in Central and South-eastern United States (CSUS). The most important bridge components for a highway bridge are depicted in Figure 5.1 and can categorized into three categories as follows:

- Superstructure: The components of a bridge that directly receive the live load comprise the superstructure. These components typically consist of bridge girders,

deck, parapet, etc. In this study, it's assumed that the bridge superstructure remains within the linear range during an earthquake event, hence, it's nonlinear properties are not considered.

- Substructure: These are the components that support the bridge and transfer all the load from the superstructure and substructure to the surrounding soil. The substructure comprises of bent, columns, foundations and abutments.
- Bearings: Bearings are mechanical devices that allow the interaction between substructure and superstructure so that the load from the superstructure can be transferred to the substructure.

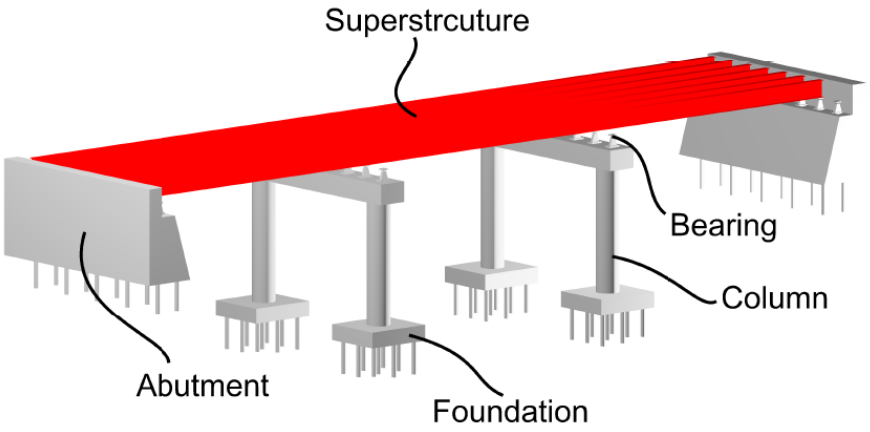


**Figure 5.1 – Typical Bridge Configuration**

The three dimensional analytical models are generated using open source finite element package OpenSees (Mazzoni et al. 2006). This package is preferred for the study as it permits users a flexibility to generate components with a great degree of accuracy and to evaluate the response of bridge components in detail. The response at component-level is studied in transverse and longitudinal direction and combined using the square root of the sum of square roots technique (SRSS). The major components studied are columns and

bearings. The following subsections outline the model of the representative bridge for the four multi-span bridge classes.

## 5.2 Deterministic Seismic Response

Deterministic seismic analysis helps to determine the bridge response at the component level due to inclusion of a lap splice. The Rayleigh damping assumed for all the models is 5%. The deterministic response is evaluated using a single ground motion from Rix and Fernandez-Leon (2004) ground motions. Figure 5.2 depicts the acceleration-time history plots of the selected ground motion. This ground motion has the maximum PGA of 0.36g and duration equal to about 13 seconds. This ground motion is chosen to simulate the effect of expected maximum PGA for Site Class E in Georgia which is equal to 0.35g.

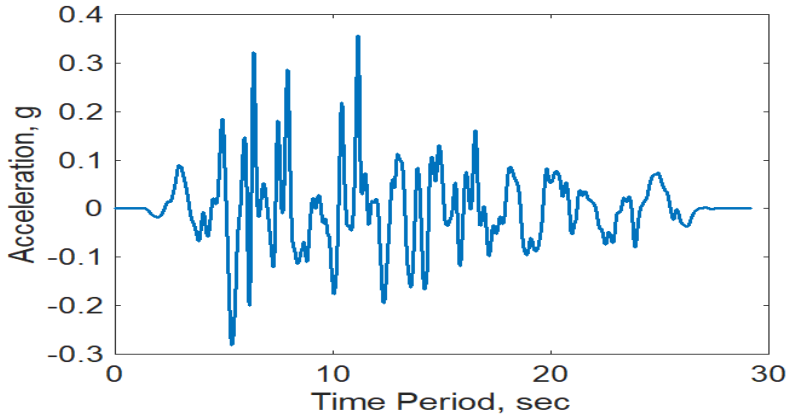


**Figure 5.2 – Acceleration-Time Plot for Rix Ground Motion Selected for Deterministic Bridge Analysis.**

### *5.2.1 Multi-Span Simply Supported Concrete Girder Bridge*

#### 5.2.1.1 Superstructure

Multi-span simply supported concrete girder bridge class comprises about 41% of bridges in the state of Georgia. Figure 5.3 presents the basic geometric layout for the multi-span simply supported concrete girder bridge. The bridge has 3 spans which are 67’-6’’, 75’ and 67’-6’’ long. The deck of the bridge is 43’-11’’ wide and uses an 8’’ thick concrete slab supported by 5 AASHTO Type III PSC beam girders on Spans 1 and 2 and AASHTO Type II PSC beam girders on Span 3. The gaps present at the adjacent spans is 4’’, whereas at the abutments, the gaps are equal to 2’’.

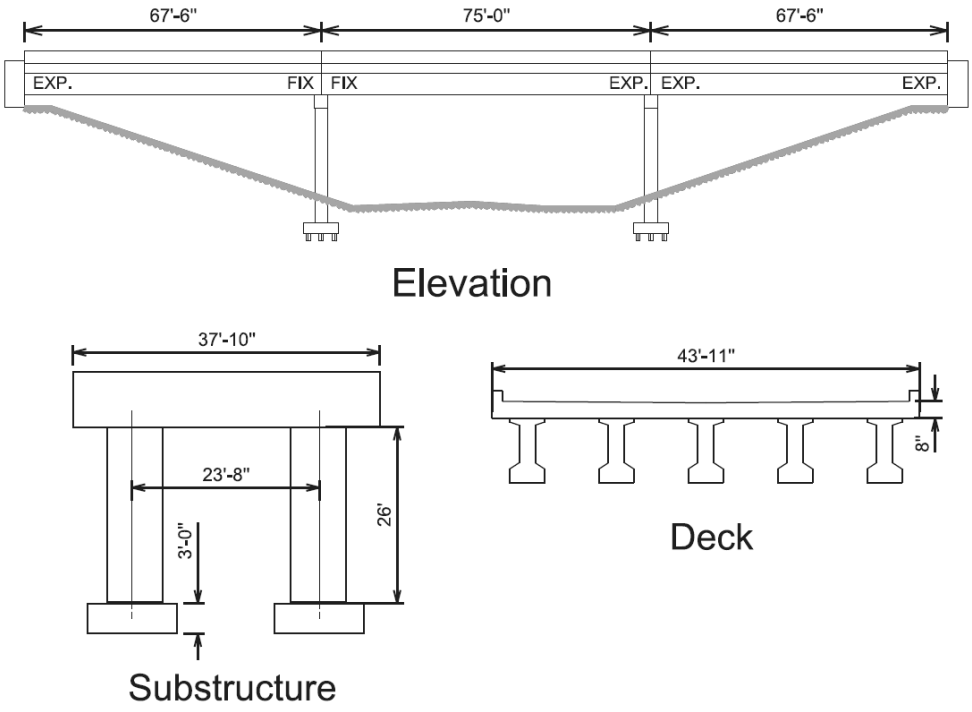


**Figure 5.3 – Multi-Span Simply Supported Concrete Girder Bridge Layout.**

5.2.1.2 Substructure

The substructure is made of 37’10’’ wide 2-column concrete bents. As illustrated in Figure 5.4, the bent beam has a square cross-section with an edge length of 3’6’’ which

is supported by 3’ by 3’ square columns. The bent beam uses 5 equally spaced #11 bars on top and bottom edges and 3 equally spaced #5 bars on the side edges with a minimum clear concrete cover of 2’’ with #4 bars for transverse reinforcement spaced at a maximum distance of 12’’. The two supporting columns for each bent have a center-to-center distance of 23’8’’ and use reinforcement detailing of 12 #11 bars equally spaced rebars with a transverse reinforcement being #4 bars spaced at 12’’. The average height of the columns is 26’ on average and the lap splice extends 9’ from the base of the column. The columns are supported by standard HP 14 × 73 steel H piles.

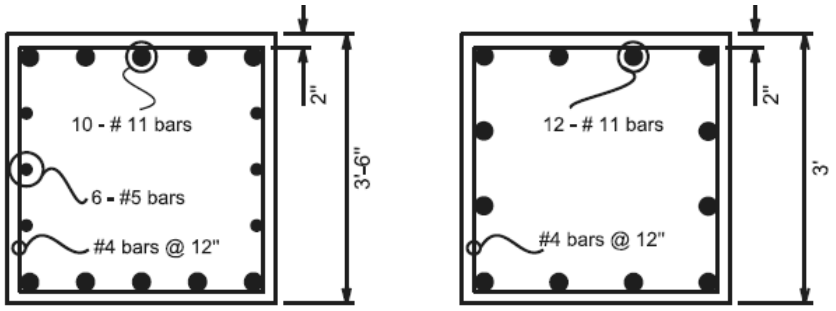


**Figure 5.4 – Cross-Sectional Layout for Bent Beam and Column for Multi-Span Simply Supported Concrete Girder Bridge.**

5.2.1.3 Bearings

Laminated elastomeric bearings are the most commonly used bearings for MSSS concrete bridge class. These bearings have a dowel bar embedded in the concrete bent which extends into the bridge girder as shown in Figure 5.5. The elastomeric pad is reinforced using steel plates that are placed in between the layers of elastomer to reduce bulging and shear strains in the pad. Although the steel layers increase the compressive and flexural stiffness of the bearing pad, however, there is no significant change in the shear

stiffness (Roeder and Stanton, 1983). The behavior of these bearings is characterized by sliding of the girder over the elastomeric pad. Initially, there exists a gap between the girder and dowel bar as illustrated in Figure 5.5. The friction between the elastomer and girder provides the initial stiffness for sliding until the movement is enough to fill the gap between the dowel bar and girder. At this point, the resistance to the sliding motion is provided by the combined action of the elastomeric pad and the dowel bar.

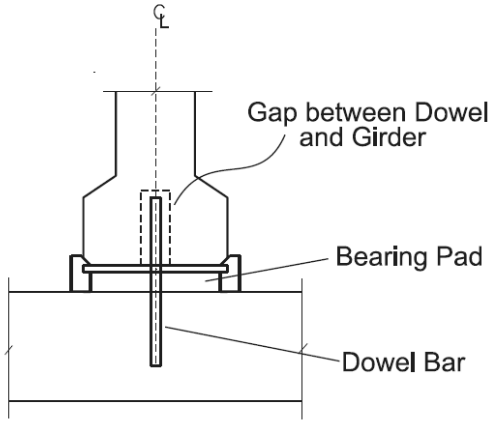


**Figure 5.5 – Typical Layout of Elastomeric Bearing**

The initial stiffness provided by the elastomeric pad is modelled as elastic perfectly plastic material as shown in Figure 5.6(a). Choi (2002) proposed a formulation for calculating the initial stiffness $k_0$ of the bearing as follows:

$$k_0 = \frac{GA}{h_r} \tag{14}$$

where $G$ is the shear modulus of the elastomer, $A$ is the area of the elastomeric pad, and $h_r$ is the height of the bearing pad. The area and height of the elastomeric pad are dependent on the bearing configuration, and the shear modulus of the elastomer is taken as 131.57 pounds/sq. in.

The frictional coefficient between the concrete girder and elastomeric pad governs the yield force that can be developed in the bearing pad. Experimental tests conducted on elastomeric bearings have revealed that the coefficient of friction is a function of the normal stress imposed by the superstructure on the bearing. Based on experimental tests, Scharge (1981) proposed an empirical formula to determine the frictional coefficient $\mu$ as follows:

$$\mu = 0.05 + \frac{0.4}{\sigma_m} \tag{15}$$

where $\sigma_m$ is the normal stress on the bearing pad due to the superstructure.

As the gap between the dowel bar and girder is filled, the dowel bar is engaged in the bearing sliding motion. The behavior of the dowel bars can be characterized as lateral force acting on a cantilever. Initially, when the dowel bar is in the elastic range, it's assumed to behave linearly. Under moderate to high lateral loads, the bar follows a nonlinear pattern until the fracturing of the bars which leads to a sudden drop in the strength. Although the diameter of the dowel bars used for elastomeric bearings in Georgia is 1 1/4'', dowel bars in the present study are assumed to be 1'' in diameter due to lack of research done on the response of dowel bars. Choi (2002) evaluated the response of 1'' diameter dowel bars using an ABAQUS model. The stress-strain behavior of the dowel bar, as shown in Figure 5.6(b), used in the present study is taken from his work with the same stiffness values.

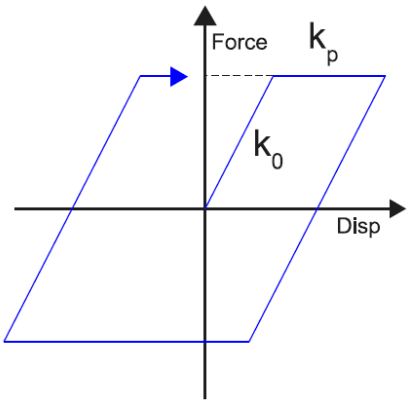


**Figure 5.6(a)**

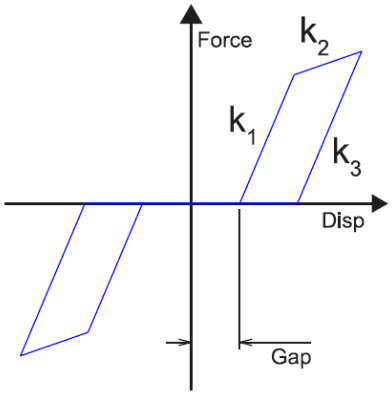


**Figure 5.6(b)**

**Figure 5.6 – Stress-Strain Model Used for (a) Elastomeric Pad, and (b) Dowel Bar in the Elastomeric Bearing.**

5.2.1.4 Seismic Response

The effect of lap splice and transverse reinforcement spacing on the main components of the bridge is analyses through the means of nonlinear time history analysis. Due to the presence of a lap splice at the base of the column, more demand is imposed on the bridge columns. The demand is further increased when the lap splice is provided with non-seismic column transverse spacing. This phenomenon is illustrated in Figure 5.7, which shows about 32% increase in the curvature demand when the lap splice is provided with non-seismic transverse reinforcement spacing and about 19% increase in the when the lap splice is provided with seismic transverse reinforcement spacing.

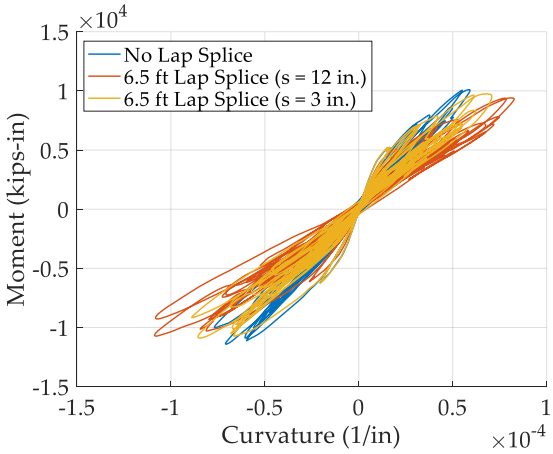


**Figure 5.7 – Curvature Demand on Column Base of MSSS Concrete Bridge.**

The comparative force-displacement curves for the fixed and expansion laminated elastomeric bearings in the bridge are shown in Figure 5.8. For the fixed bearings, the gap between the dowel bar and elastomeric pad is 0.12 inches. Figure 5.8(a) shows the change in stiffness of the force-displacement curve of the fixed elastomeric bearing due to engagement of the dowel bar. Similarly, for the expansion bearing, the gap is 1.0 inch as shown in Figure 5.8(b). The bearing response for all the three cases is similar because the chosen ground motion is not of a very high intensity.

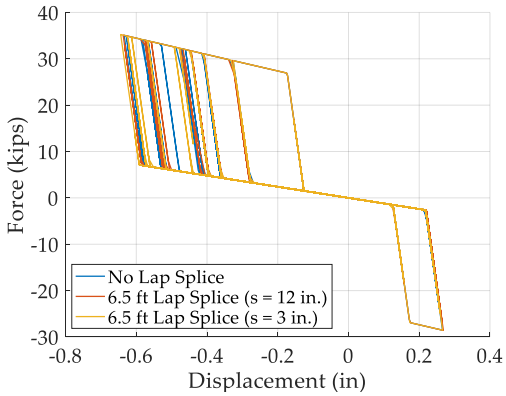


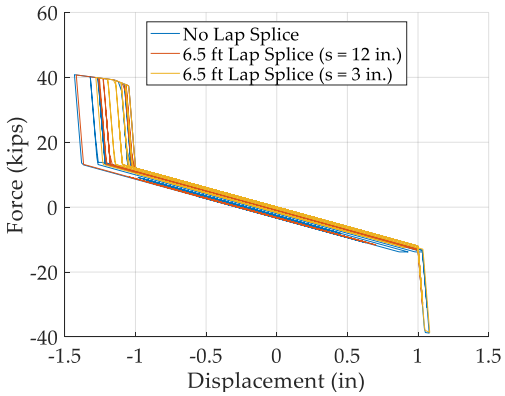


**Figure 5.8(a)** **Figure 5.8(b)**

**Figure 5.8 – Force-Displacement Curves for (a) Fixed (b) Expansion Laminated Elastomeric Bearings Used in MSSS Concrete Bridge.**

### *5.2.2 Multi-Span Continuous Steel Girder Bridge*

#### 5.2.2.1 Superstructure

The next bridge class considered in the study was multi-span continuous type steel girder bridges. These bridges are about comprise about 11% bridges in Georgia. The basic geometric configuration for a representative bridge from this bridge class is shown in Figure 5.9. The bridge consists of 3 spans and is 36’-10’’ wide. The span lengths for this bridge are 43’, 67’ and 43’. The deck is a composite steel deck supported by 5 wide flange steel girders.

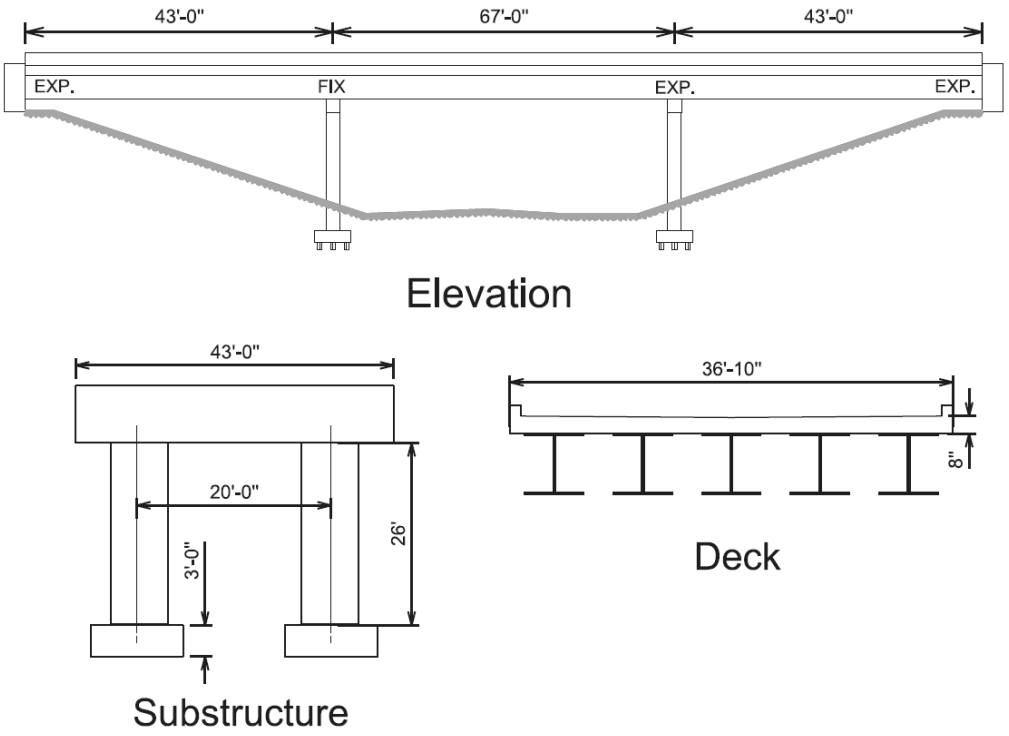


**Figure 5.9 – Multi-Span Continuous Steel Girder Bridge Layout.**

5.2.2.2 Substructure

Like the previous bridge class, the substructure consists of 2-column bents. The average width of the bents is 43’ and the average height of the columns is 26’. The columns are spaced at a distance of 20’. The lap splice is present at the base of the column and has a length of 6.5’. The cross-sectional layouts for the bent and column are shown in Figure 5.10. The bent has a square cross-section with each side equal to 3’ and is reinforced with 7 #11 bars each at the top and bottom edges and 2 #4 bars on each side. The shear reinforcement for the bents is provided by #5 bars are 12’’ spacing. Likewise, the column has a square cross-section with the edge length equal to 3’. The column reinforcement consists of 12 #12 equally spaced bars and #4 stirrups spaced at 12’’.

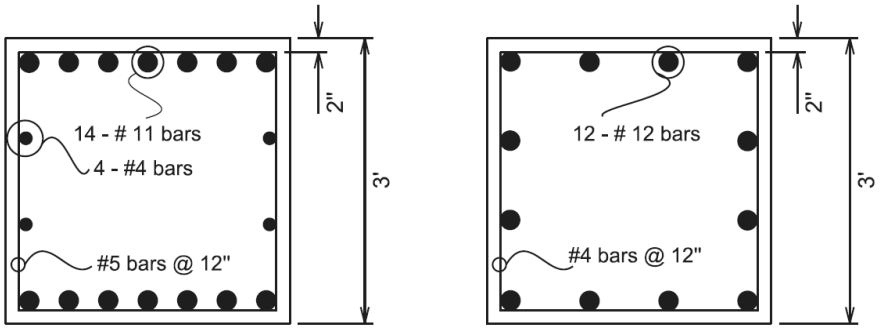


**Figure 5.10 – Cross-Sectional Layout for Bent Beam and Column for Multi-Span Continuous Steel Girder Bridge.**

5.2.2.3 Bearings

Low-profile steel bearings are the second most commonly used bearings for steel bridges in Georgia. A prototype of low-profile bridge bearings is shown in Figure 5.11. These bearings are constructed by attaching a masonry plate to the top of the bent or abutment using anchor bolts and a sole plate underneath the girder. For fixed bearings, a curved sole plate and pintles are provided to restrict the translational movements while maintaining the rotational movement. On the other hand, for expansion bearings, no pintles are provided so that free translational movement is permitted to dissipate the energy.

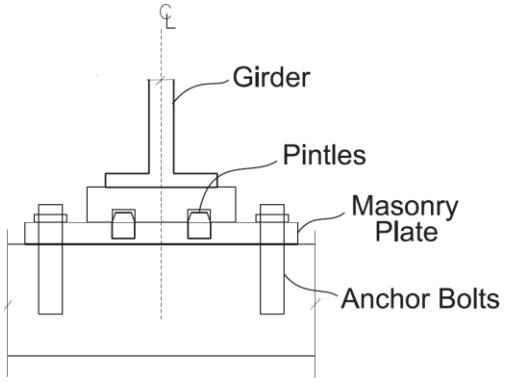


**Figure 5.11 – Typical Layout of Low-Profile Steel Fixed Bearing**

The study on analytical modelling of bridge steel bearings was initiated by Mander et al. (1996), however, the test apparatus used by them was not appropriate to simulate the

field conditions as the test bearings were mounted to steel assemblies to constrain the damage only to the pintles. This is in contrast with the field conditions where the masonry plate is attached to the concrete pedestal by the means of anchor bolts. Thus, failure mechanism of either the anchor bolt or pintle, whichever happens first could lead to the bearing failure. Based on this, Steelman et. al. (2013) considered two types of low-profile steel fixed bearings: weak anchor and weak pintles. They investigated the cyclic response of these bearings through an improved test apparatus to formulate more accurate analytical models. For the representative MSC steel bridge in Georgia, the diameter of the anchor and pintle is equal to 1 in., however, the effective diameter of the anchor bolts is reduced to $4/5^{th}$ of the original diameter due to the thread adjustment factor. Due to this, the bearings used in Georgia are considered to be weak anchor bearings and the failure is governed by the rupturing of the anchor bolts.

The fuse capacity $V_{fuse}$ for steel bearings can be calculated as per the following equation (IDOT, 2009):

$$V_{fuse} = \phi n 0.6 F_u A_b$$

where $\phi$ is the strength reduction factor (equal to unity), $n$ is the number of shear transfer elements (equal to 2 as there are two anchors), $F_u$ is the ultimate tensile strength of the material, $A_b$ is the effective cross-sectional area of the shear element.

Along with the fusing action, the bearing interface provides resistance to the translational movement through frictional force. Like elastomeric bearings, frictional resistance is modeled as elastic perfectly plastic and is coupled with the anchor bolt backbone curve in parallel.

According to the latest AASTHO Specifications (2014), the use of steel bearings is recommended only as fixed bearings whereas expansion steel bearings have become obsolete. However, as the representative bridge is an old bridge, steel bearings have been used as expansion bearings too. The only difference between fixed and expansion bearing is that there are no pintles to restrict the translational movement in the latter.

#### 5.2.2.4 Seismic Response

Figure 5.12 shows the effect of the 9-ft. lap splice and transverse reinforcement spacing on the curvature demand imposed on the MSC steel girder bridge column. As the ground motion is of medium PGA intensity, the column response mostly remains in the linear range. A decrease in the moment capacity and increase in the curvature demand on the column can be observed from the figure when the lap splice is present at the base of the column. The increase in curvature is approximately 12.12% when non-seismic transverse spacing is provided and 3.93% when seismic reinforcement spacing is provided.

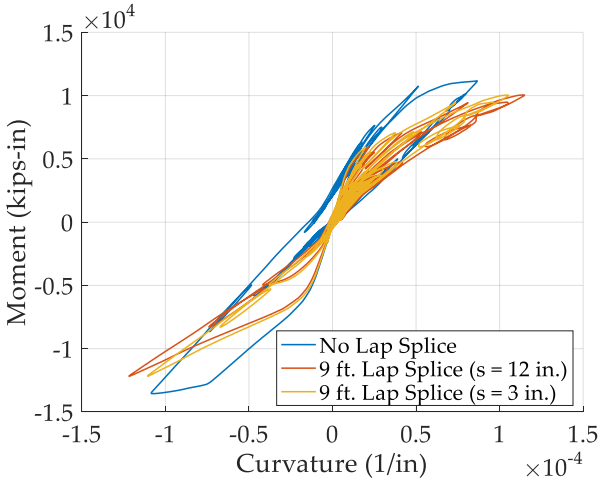


**Figure 5.12 – Curvature Demand on Column Base of MSC Steel Girder Bridge.**

The force-displacement response for the fixed and expansion steel bearings for MSC steel girder bridge is shown in Figure 5.13(a) and Figure 5.13(b), respectively.

Similar to the previous bridge class, the bearing responses are very similar. The force-displacement response for both types of bearings stays in the linear range which indicates that there was no rupture in either pintles or anchors.

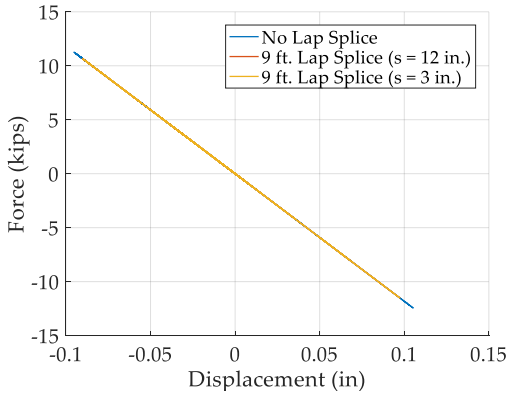


**Figure 5.13(a)**

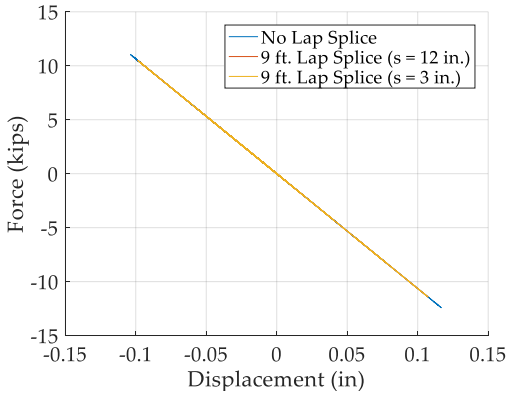


**Figure 5.13(b)**

**Figure 5.13 – Force Force-Displacement Curves for (a) Fixed (b) Expansion Steel Bearings Used in MSC Steel Girder Bridge.**

### *5.2.3 Multi-Span Simply Supported Steel Girder Bridge*

#### 5.2.3.1 Superstructure

The next bridge class considered in the study was MSSS steel girder. The general layout for the representative bridge in this bridge class is shown in Figure 5.14. Compared to the previous two bridge classes, this bridge has a wider deck. The deck spans 62’6’’ in the transverse direction and is supported by 9 steel girders. The side spans of the bridge are 37’2’’ long whereas the main span is 67’3’’ long.

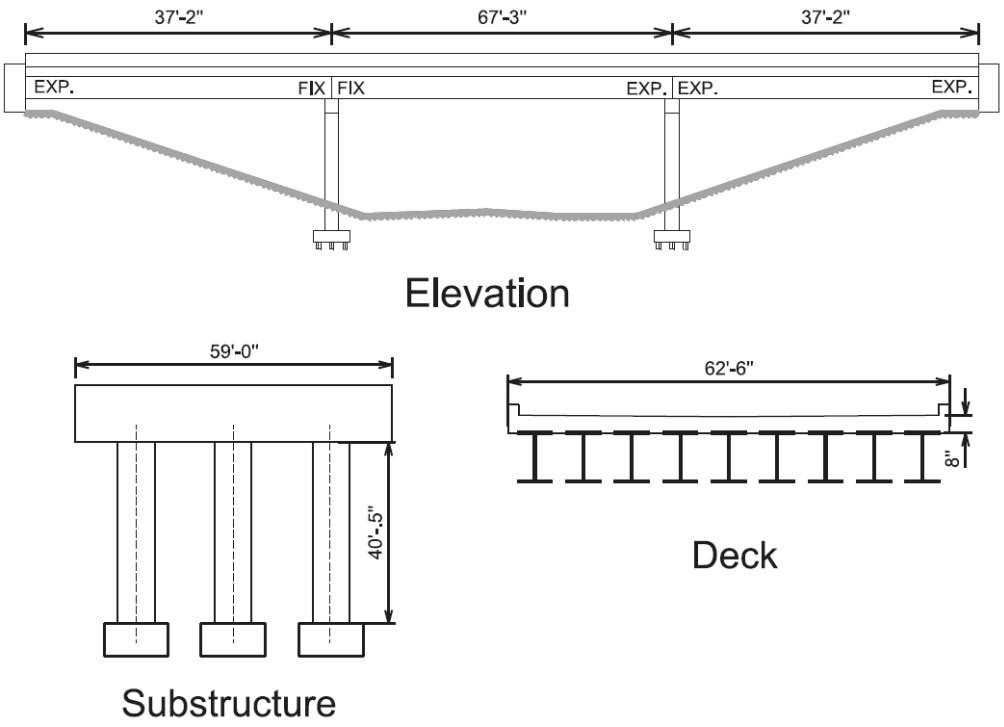


**Figure 5.14 – Multi-Span Simply Supported Steel Girder Bridge Layout.**

5.2.3.2 Substructure

The substructure for this bridge is supported by two 3-column bents. Due to a wider deck, the width of the deck is 59’ and the average height of the 3 columns is 13’. The bent cross-section is a rectangular cross-section with width equal to 3’ and depth equal to 3’6’’. The bent is reinforced with 14 #11 bars on the top and bottom edges and 2 #6 bars on the side edges. The shear reinforcement comprises #5 bars spaced at 12’’ with a clear concrete cover of 2’’. Figure 5.15 depicts the column cross-section which is a square with the edge length equal to 3’. The column section is reinforced with 8 equally spaced #11 bars with #4 bars providing the shear reinforcement at 12’’ spacing. Although the actual lap splice length in the plans for this bridge is equal to 4.25’’, the lap splice length is taken equal to

6.5’’. This is done because currently GDOT doesn’t construct bridges with such short lap splice lengths.

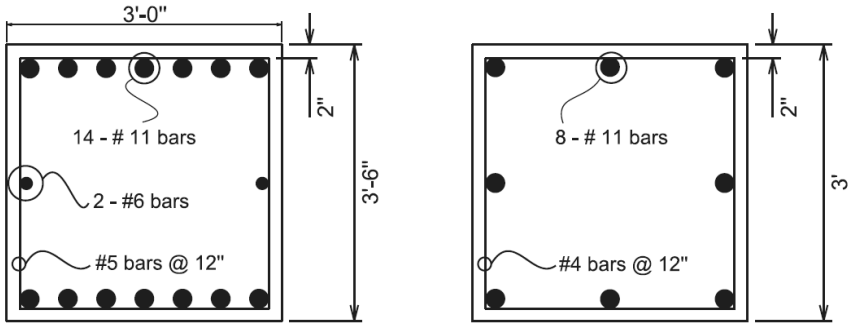


**Figure 5.15 – Cross-Sectional Layout for Bent Beam and Column for Multi-Span Simply Supported Steel Girder Bridge.**

5.2.3.3 Bearings

As stated in Section 5.2.2.3, the commonly used bearing for steel bridges in Georgia is low profile steel bearings. This bridge class uses the same type of bearing, as well. Currently, GDOT does not use

5.2.3.4 Seismic Response

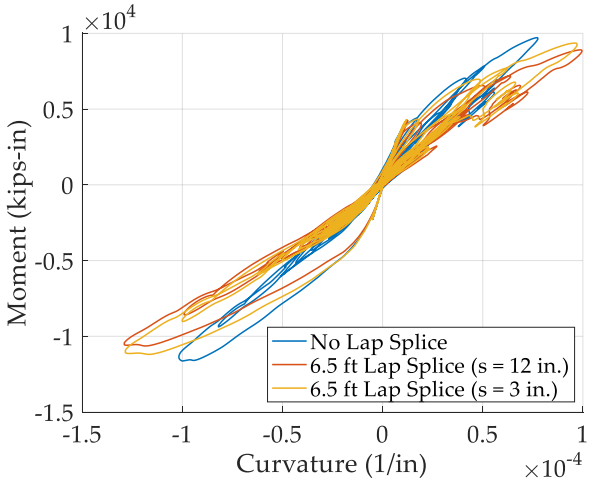


**Figure 5.16 – Curvature Demand on Column Base of MSSS Steel Girder Bridge.**

For the MSSS steel bridge, there is more displacement demand imposed compared to the MSC steel bridge. This could be due to the more inertial mass in the superstructure of the MSSS steel bridge. Due to this, the anchor bolt of the fixed bearing fails at displacement approximately equal to 0.4 inches for all the three cases as shown in Figure 5.17(a). After the rupture of the anchor bolt, the bearing response is governed by the friction between the bent and masonry plate. As shown in Figure 5.17(b), the displacement response for the expansion steel bearings is governed by friction only as there is no anchor bolt contributing to the stiffness.

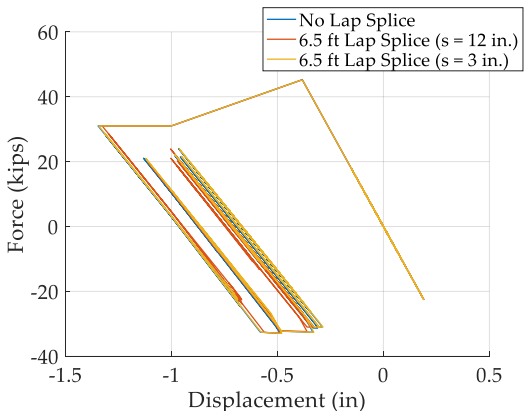


**Figure 5.17(a)**

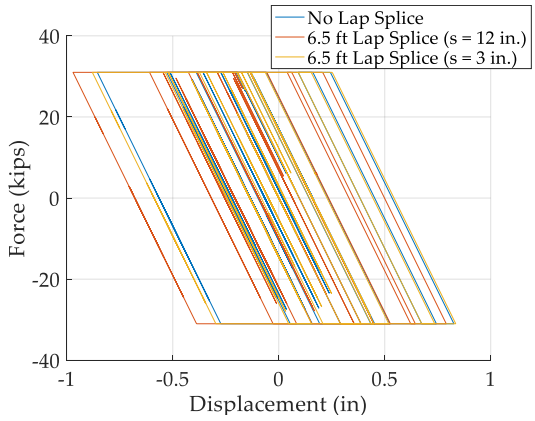


**Figure 5.17(b)**

**Figure 5.17 - Force-Displacement Curves for (a) Fixed (b) Expansion Steel Bearings Used in MSSS Steel Girder Bridge.**

# CHAPTER 6. SITE-SPECIFIC FRAGILITY CURVES

With the objective of assessing demands imposed on different bridge components, this chapter presents PSDMs for multi-highway bridge classes in Georgia. These curves are generated based on nonlinear dynamic analyses under a number of ground motions as a function of peak ground acceleration (PGA) and seismic detailing requirements. Furthermore, fragility curves at component- and system-level for these bridges are presented in the next subsection. Based on these curves, site-specific seismic damage risk is evaluated for Seismic Classes A, B, C, D and E.

## 6.1 PSDMs for Multi-Span Highway Bridges

As discussed in Section 4.3, Probabilistic Seismic Demand Models (PSDMs) are generated for columns based on the maximum curvature ductility demands on them. A suite of 48 ground motions are used to assess the demand quantity of interest. PSDMs for various classes of bridges are plotted in Figure 6.1 – Probabilistic Seismic Demand Models (PSDMs) for Column Curvature Ductility Demand for (a) MSSS Concrete Bridge, (b) MSC Steel Girder Bridge, and (c) MSSS Steel Girder Bridge. PSDMs are plotted on a log-log scale with the demand variable on the y-axis and intensity measure on the x-axis. The PSDMs reveal the deficiency in seismic performance for all the three bridge classes when the logarithm of PGA is greater than -2.

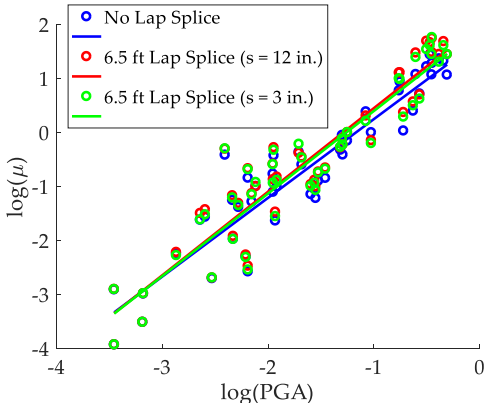


**Figure 6.1 (a)**

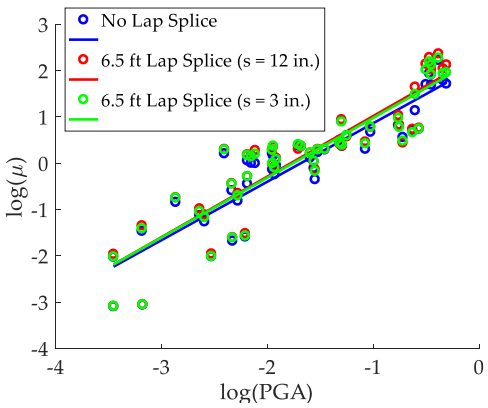


**Figure 6.1 (b)**

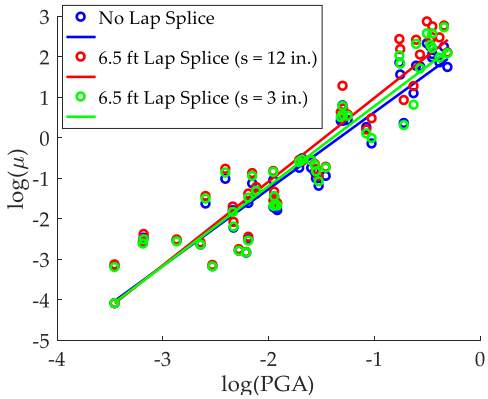


**Figure 6.1 (c)**

**Figure 6.1 – Probabilistic Seismic Demand Models (PSDMs) for Column Curvature Ductility Demand for (a) MSSS Concrete Bridge, (b) MSC Steel Girder Bridge, and (c) MSSS Steel Girder Bridge**

## 6.2 Seismic Fragility Curves and Site Specific Risk Estimates

The following subsections present the column seismic fragility curves for the four limit states considered in this study. These curves are presented for three cases for transverse spacing and lap splice: 1) no lap splice, 2) lap splice at the bottom of the column with a non-seismic transverse spacing (12 in. spacing), and 3) lap splice at the bottom of the column with a non-seismic transverse spacing (3 in. spacing).

### *6.2.1 Multi-Span Simply Supported Concrete Bridges*

Figure 6.2 represents the fragility curves for all the limit states for these three cases.

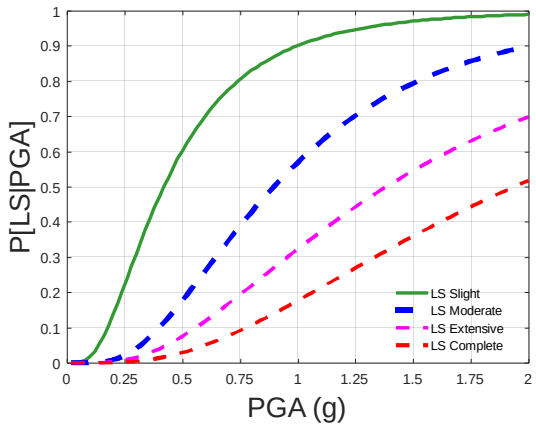


**Figure 6.2 (a)**

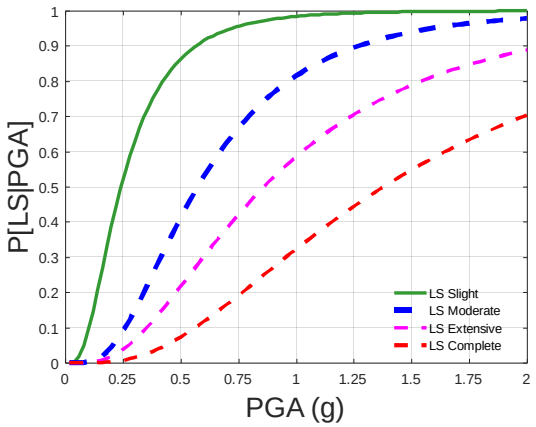


**Figure 6.2 (b)**

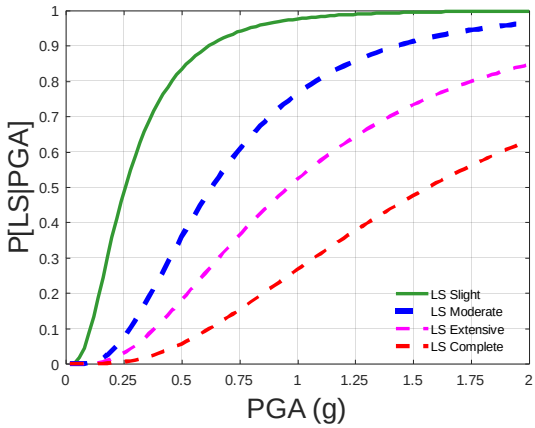


**Figure 6.2 (c)**

**Figure 6.2 – Seismic Fragility Curves for MSSS Concrete Class for (a) No-Lap Splice with Seismic Spacing (s = 3 in.), (b) Lap Splice with Seismic Spacing (s = 3 in.), and (c) Lap Splice with Seismic Spacing (s = 12 in.).**

**Table 6-1 – Comparative Probability Estimates of Exceeding Four Limit States for MSSS Concrete Bridges for (a) No-Lap Splice with Seismic Spacing (s = 3 in.), (b) Lap Splice with Seismic Spacing (s = 3 in.), and (c) Lap Splice with Seismic Spacing (s = 12 in.).**

**Table 6-1(a)**

| PGA (g) | LS 1 | LS 2 | LS 3 | LS 4 |
|---|---|---|---|---|
| 0.05 | 0.0% | 0.0% | 0.0% | 0.0% |
| 0.10 | 1.7% | 0.0% | 0.0% | 0.0% |
| 0.15 | 6.4% | 0.2% | 0.1% | 0.0% |
| 0.20 | 13.6% | 0.85% | 0.31% | 0.07% |
| 0.25 | 22.1% | 2.10% | 0.77% | 0.20% |
| 0.30 | 30.9% | 4.07% | 1.52% | 0.44% |
| 0.35 | 39.4% | 6.7% | 2.6% | 0.8% |

**Table 6-1(b)**

| PGA (g) | LS 1 | LS 2 | LS 3 | LS 4 |
|---|---|---|---|---|
| 0.05 | 0.9% | 0.0% | 0.0% | 0.0% |
| 0.10 | 9.2% | 0.2% | 0.1% | 0.0% |
| 0.15 | 23.6% | 1.5% | 0.6% | 0.0% |
| 0.20 | 38.8% | 4.4% | 1.8% | 0.3% |
| 0.25 | 52.0% | 8.9% | 3.7% | 0.7% |
| 0.30 | 62.8% | 14.8% | 6.4% | 1.5% |
| 0.35 | 71.1% | 21.2% | 9.7% | 2.5% |

**Table 6-1(c)**

| PGA (g) | LS 1 | LS 2 | LS 3 | LS 4 |
|---|---|---|---|---|
| 0.05 | 0.0% | 0.0% | 0.0% | 0.0% |
| 0.10 | 0.2% | 0.0% | 0.0% | 0.0% |
| 0.15 | 2.2% | 0.0% | 0.0% | 0.0% |
| 0.20 | 8.7% | 0.3% | 0.0% | 0.0% |
| 0.25 | 19.5% | 1.3% | 0.2% | 0.1% |
| 0.30 | 32.7% | 3.6% | 0.7% | 0.4% |
| 0.35 | 45.9% | 7.6% | 1.6% | 0.9% |

6.2.1.1 Site Class A

Table 6-2 – Seismic represents the failure probabilities of the column reaching or exceeding each limit state. The maximum probability of exceeding Limit State 1 is

estimated to be equal to 6.23% in Region 1. As all the probabilities are quite low, 6.5' lap splices with non-seismic transverse spacing are safe to be used for this Site Class A.

**Table 6-2 – Seismic Risk for MSSS Concrete Bridges for Site Class A when Lap-Splice with Non-Seismic Spacing is Provided.**

| Region | Zone | PGA (g) | Limit State 1 | Limit State 2 | Limit State 3 | Limit State 4 |
|---|---|---|---|---|---|---|
| 1 | 1-A | 0.13 | 6.23% | 0.07% | 0.03% | 0.00% |
| 2 | 1-A | 0.11 | 3.57% | 0.02% | 0.01% | 0.00% |
| 3 | 1-A | 0.08 | 0.66% | 0.00% | 0.00% | 0.00% |
| 4 | 1-A | 0.06 | 0.17% | 0.00% | 0.00% | 0.00% |
| 5 | 1-A | 0.05 | 0.02% | 0.00% | 0.00% | 0.00% |
| 6 | 1-A | 0.03 | 0.00% | 0.00% | 0.00% | 0.00% |

#### 6.2.1.2 Site Class B

Although for Site Class B, the whole state falls in Seismic Zone 1-A, the earthquake intensities for each region are higher than those for Site Class A. This results in higher probabilities for Site Class B compared to Site Class A, as evident from Table 6-3. The maximum probability of exceeding the first limit state is 13.83% seen for Region 1. To be on the conservative side, lap splice with seismic reinforcement spacing could be provided for Region 1 for Site Class B, however, for the rest of the state, a lap splice with a non-seismic spacing will be conservative enough.

**Table 6-3 – Seismic Risk for MSSS Concrete Bridges for Site Class B when Lap-Splice with Non-Seismic Spacing is Provided.**

| Region | Zone | PGA (g) | Limit State 1 | Limit State 2 | Limit State 3 | Limit State 4 |
|---|---|---|---|---|---|---|
| 1 | 1-A | 0.16 | 13.83% | 0.36% | 0.14% | 0.01% |
| 2 | 1-A | 0.14 | 8.76% | 0.14% | 0.06% | 0.00% |
| 3 | 1-A | 0.10 | 2.11% | 0.01% | 0.01% | 0.00% |
| 4 | 1-A | 0.08 | 0.66% | 0.00% | 0.00% | 0.00% |
| 5 | 1-A | 0.06 | 0.11% | 0.00% | 0.00% | 0.00% |
| 6 | 1-A | 0.04 | 0.01% | 0.00% | 0.00% | 0.00% |

6.2.1.3 Site Class C

As observed from Table 6-4(a) when a lap splice with non-seismic spacing is provided at the base of the columns, the probabilities of exceeding Limit State 1 for Seismic Zone 1-B (Regions 1 & 2) are 23.51% and 16.11%. Table 6-4(b) presents the probabilities for Regions 1 & 2 when a lap splice with seismic spacing is provided at the base of the column. Even when the seismic spacing is provided, the probabilities for Regions 1 and 2 are still 22.01% and 15.02% which are still on the higher side. Table 6-4(c) presents the probabilities for Regions 1 & 2 when no lap splice is provided at the base of the column. In this case, there is a significant reduction in the probabilities as they drop down to 5.79% and 3.36%. Not providing a lap splice at the base of the column for Seismic Zone 1-B leads to reduction of probabilities by 17.72% and 12.75%. Hence, for Site Class C, it is recommended that the lap splice should not be provided at the base of the column for MSSS Concrete bridge class when the bridge is in Seismic Zone 1-B.

**Table 6-4 – Seismic Risk for MSSS Concrete Bridges for Site Class C when (a) Lap-Splice with Non-Seismic Spacing is Provided, (b) Lap-Splice with Seismic Spacing is Provided, and (c) No Lap Splice is Provided**

| Region | Zone | PGA (g) | Limit State 1 | Limit State 2 | Limit State 3 | Limit State 4 |
|---|---|---|---|---|---|---|
| 1 | 1-B | 0.19 | 23.51% | 1.10% | 0.42% | 0.04% |
| 2 | 1-B | 0.17 | 16.11% | 0.49% | 0.19% | 0.01% |
| 3 | 1-A | 0.12 | 4.80% | 0.05% | 0.02% | 0.00% |
| 4 | 1-A | 0.10 | 1.73% | 0.01% | 0.00% | 0.00% |
| 5 | 1-A | 0.07 | 0.36% | 0.00% | 0.00% | 0.00% |
| 6 | 1-A | 0.05 | 0.02% | 0.00% | 0.00% | 0.00% |

| Region | Zone | PGA (g) | Limit State 1 | Limit State 2 | Limit State 3 | Limit State 4 |
|---|---|---|---|---|---|---|
| 1 | 1-B | 0.19 | 22.01% | 0.97% | 0.37% | 0.03% |
| 2 | 1-B | 0.17 | 15.02% | 0.43% | 0.17% | 0.01% |

| Region | Zone | PGA (g) | Limit State 1 | Limit State 2 | Limit State 3 | Limit State 4 |
|---|---|---|---|---|---|---|
| 1 | 1-B | 0.19 | 5.79% | 0.13% | 0.05% | 0.00% |
| 2 | 1-B | 0.17 | 3.36% | 0.05% | 0.02% | 0.00% |

6.2.1.4 Site Class D

For Site Class D, Table 6-5(a) shows that the probabilities are 40.15% and 29.38% for Regions 1 and 2, respectively, when the lap splice with non-seismic spacing is provided. The probabilities for Regions 1 and 2 when lap splice is not provided at the column base are shown in Table 6-5(b) and a reduction of 26.99% for Region 1 and 21.31% for Region

2 for Limit State 1 is observed. Due to this considerable reduction in the probabilities, it is recommended that the lap splice should not be provided for Seismic Zone 2 for Site Class D.

Although for the rest of the state, the risk estimates are low because of lower earthquake intensities even though it falls in Zone 1-B, it is recommended that seismic spacing requirements should be followed for Seismic Zone 1-B.

**Table 6-5 – Seismic Risk for MSSS Concrete Bridges for Site Class D when (a) Lap-Splice with Non-Seismic Spacing is Provided, (b) Lap-Splice with Seismic Spacing is Provided for Zone 1-B and No Lap Splice is Provided for Zone 2.**

| Region | Zone | PGA (g) | Limit State 1 | Limit State 2 | Limit State 3 | Limit State 4 |
|---|---|---|---|---|---|---|
| 1 | 2 | 0.24 | 40.15% | 3.76% | 1.43% | 0.20% |
| 2 | 2 | 0.21 | 29.38% | 1.80% | 0.68% | 0.08% |
| 3 | 1-B | 0.16 | 13.83% | 0.36% | 0.14% | 0.01% |
| 4 | 1-B | 0.13 | 6.62% | 0.08% | 0.04% | 0.00% |
| 5 | 1-B | 0.09 | 1.73% | 0.01% | 0.00% | 0.00% |
| 6 | 1-A | 0.06 | 0.17% | 0.00% | 0.00% | 0.00% |

| Region | Zone | PGA (g) | Limit State 1 | Limit State 2 | Limit State 3 | Limit State 4 |
|---|---|---|---|---|---|---|
| 1 | 2 | 0.24 | 13.16% | 0.60% | 0.22% | 0.04% |
| 2 | 2 | 0.21 | 8.07% | 0.24% | 0.09% | 0.01% |
| 3 | 1-B | 0.16 | 12.89% | 0.32% | 0.13% | 0.01% |
| 4 | 1-B | 0.13 | 6.15% | 0.08% | 0.03% | 0.00% |
| 5 | 1-B | 0.09 | 1.62% | 0.01% | 0.00% | 0.00% |

6.2.1.5 Site Class E

Table 6-6(a) presents the seismic risk estimated for MSSS concrete bridge class for Site Class E when the lap splice is provided at the base of the column. These numbers are on the higher end. Eliminating the lap splice reduces the probabilities by 34.66% for Region 1. There is substantial reduction of probabilities for other regions as well as can be observed from Table 6-6(b). Due to this, it would be best to provide no lap splice at the base of the column for Site Class E.

**Table 6-6 – Seismic Risk for MSSS Concrete Bridges for Site Class E when (a) Lap-Splice with Non-Seismic Spacing is Provided, (b) Lap-Splice with Seismic Spacing is Provided for Zone 1-B and No Lap Splice is Provided for Zone 2.**

| Region | Zone | PGA (g) | Limit State 1 | Limit State 2 | Limit State 3 | Limit State 4 |
|---|---|---|---|---|---|---|
| 1 | 2 | 0.35 | 68.53% | 16.19% | 6.81% | 1.41% |
| 2 | 2 | 0.28 | 51.39% | 7.06% | 2.76% | 0.44% |
| 3 | 2 | 0.25 | 42.37% | 4.29% | 1.64% | 0.23% |
| 4 | 2 | 0.20 | 26.10% | 1.38% | 0.52% | 0.06% |
| 5 | 2 | 0.15 | 11.17% | 0.23% | 0.09% | 0.01% |
| 6 | 1-B | 0.10 | 2.11% | 0.01% | 0.01% | 0.00% |

| Region | Zone | PGA (g) | Limit State 1 | Limit State 2 | Limit State 3 | Limit State 4 |
|---|---|---|---|---|---|---|
| 1 | 2 | 0.35 | 33.87% | 4.02% | 1.46% | 0.39% |
| 2 | 2 | 0.28 | 19.88% | 1.33% | 0.48% | 0.11% |
| 3 | 2 | 0.25 | 14.36% | 0.71% | 0.26% | 0.05% |
| 4 | 2 | 0.2 | 6.76% | 0.17% | 0.07% | 0.01% |
| 5 | 2 | 0.15 | 2.03% | 0.02% | 0.01% | 0.00% |
| 6 | 1-B | 0.10 | 1.97% | 0.01% | 0.00% | 0.00% |

### *6.2.2 Multi-Span Continuous Steel Bridges*

Seismic analysis of this bridge class is done using the same set of ground motions and same lap splice cases as the previous bridge class. Fig 4.3 presents the seismic fragility curves for MSC Steel bridge class.

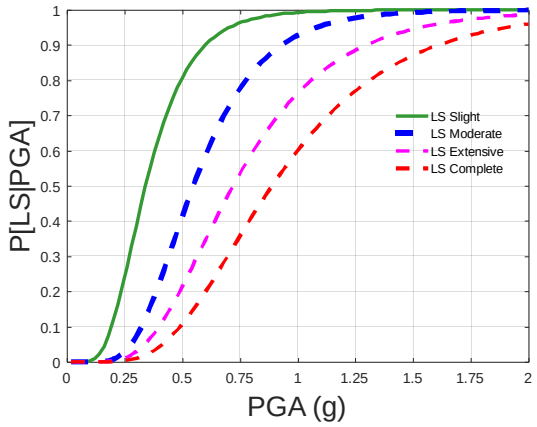


**Figure 6.4 (a)**

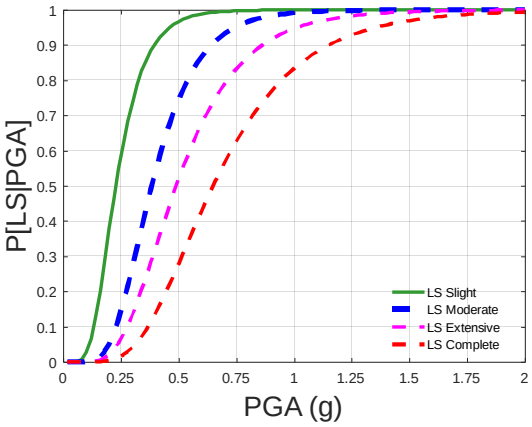


**Figure 6.4(b)**

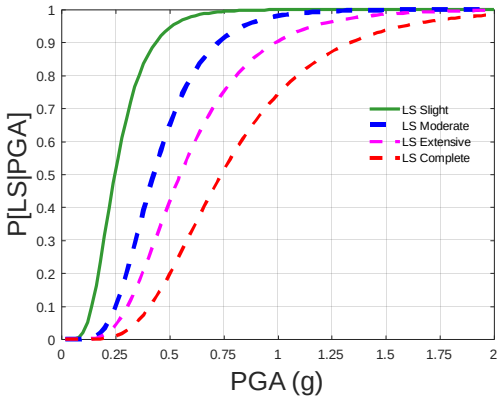


**Figure 6.4 (c)**

**Figure 6.3 - Seismic Fragility Curves for MSC Steel Class for (a) No-Lap Splice with Seismic Spacing (s = 3 in.), (b) Lap Splice with Seismic Spacing (s = 3 in.), and (c) Lap Splice with Seismic Spacing (s = 12 in.).**

**Table 6-7 – Comparative Probability Estimates of Exceeding Four Limit States for MSC Steel Bridges for (a) No-Lap Splice with Seismic Spacing (s = 3 in.), (b) Lap Splice with Seismic Spacing (s = 3 in.), and (c) Lap Splice with Seismic Spacing (s = 12 in.).**

**Table 6-7(a)**

| PGA (g) | LS 1 | LS 2 | LS 3 | LS 4 |
|---|---|---|---|---|
| 0.05 | 0.0% | 0.0% | 0.0% | 0.0% |
| 0.10 | 1.7% | 0.0% | 0.0% | 0.0% |
| 0.15 | 6.4% | 0.2% | 0.1% | 0.0% |
| 0.20 | 13.6% | 0.85% | 0.31% | 0.07% |
| 0.25 | 22.1% | 2.10% | 0.77% | 0.20% |
| 0.30 | 30.9% | 4.07% | 1.52% | 0.44% |
| 0.35 | 39.4% | 6.7% | 2.6% | 0.8% |

**Table 6-7(b)**

| PGA (g) | LS 1 | LS 2 | LS 3 | LS 4 |
|---|---|---|---|---|
| 0.05 | 0.9% | 0.0% | 0.0% | 0.0% |
| 0.10 | 9.2% | 0.2% | 0.1% | 0.0% |
| 0.15 | 23.6% | 1.5% | 0.6% | 0.0% |
| 0.20 | 38.8% | 4.4% | 1.8% | 0.3% |
| 0.25 | 52.0% | 8.9% | 3.7% | 0.7% |
| 0.30 | 62.8% | 14.8% | 6.4% | 1.5% |
| 0.35 | 71.1% | 21.2% | 9.7% | 2.5% |

**Table 6-7(c)**

| PGA (g) | LS 1 | LS 2 | LS 3 | LS 4 |
|---|---|---|---|---|
| 0.05 | 0.0% | 0.0% | 0.0% | 0.0% |
| 0.10 | 0.2% | 0.0% | 0.0% | 0.0% |
| 0.15 | 2.2% | 0.0% | 0.0% | 0.0% |
| 0.20 | 8.7% | 0.3% | 0.0% | 0.0% |
| 0.25 | 19.5% | 1.3% | 0.2% | 0.1% |
| 0.30 | 32.7% | 3.6% | 0.7% | 0.4% |
| 0.35 | 45.9% | 7.6% | 1.6% | 0.9% |

For easier comparison between the bridge classes and lap splice cases, the probability values are also presented in Table 4-1 up to 0.35g at intervals of 0.05g.

6.2.2.1 Site Class A

For MSC steel bridges in Site Class A, the corresponding probabilities of failure for the six regions are shown in Table 6-8. Because the PGA intensities are low, the

probabilities of exceeding all the limit states are low as well. The maximum probability of exceeding any limit state happens to be in Region 1 and is equal to 5.34%. Thus, providing a long lap splice at the column base with non-seismic transverse spacing is safe for this site class.

**Table 6-8 – Seismic Risk for MSC Steel Bridges for Site Class A when Lap-Splice with Non-Seismic Spacing is Provided.**

| Region | Zone | PGA (g) | Limit State 1 | Limit State 2 | Limit State 3 | Limit State 4 |
|---|---|---|---|---|---|---|
| 1 | 1-A | 0.13 | 5.34% | 0.34% | 0.14% | 0.02% |
| 2 | 1-A | 0.11 | 2.76% | 0.12% | 0.05% | 0.01% |
| 3 | 1-A | 0.08 | 0.36% | 0.01% | 0.00% | 0.00% |
| 4 | 1-A | 0.06 | 0.07% | 0.00% | 0.00% | 0.00% |
| 5 | 1-A | 0.05 | 0.01% | 0.00% | 0.00% | 0.00% |
| 6 | 1-A | 0.03 | 0.00% | 0.00% | 0.00% | 0.00% |

#### 6.2.2.2 Site Class B

For Site Class B, as shown in Table 6-9(a), the maximum probability of exceeding any limit state happens to in Region 1 and is equal 13.47%. This probability is relatively higher than Site Class A. Hence, for Site Class B, if the bridge is in Region 1, seismic transverse spacing could be used. For the rest of the state, long lap splices with non-seismic spacing are safe.

**Table 6-9 – Seismic Risk for MSC Steel Bridges for Site Class B when (a) Lap-Splice with Non-Seismic Spacing is Provided, (b) Lap-Splice with Seismic Spacing is Provided, and (c) No Lap Splice is Provided.**

| Region | Zone | PGA (g) | Limit State 1 | Limit State 2 | Limit State 3 | Limit State 4 |
|---|---|---|---|---|---|---|
| 1 | 1-A | 0.16 | 13.47% | 1.46% | 0.62% | 0.13% |
| 2 | 1-A | 0.14 | 7.95% | 0.63% | 0.26% | 0.05% |
| 3 | 1-A | 0.10 | 1.48% | 0.05% | 0.02% | 0.00% |
| 4 | 1-A | 0.08 | 0.36% | 0.01% | 0.00% | 0.00% |
| 5 | 1-A | 0.06 | 0.04% | 0.00% | 0.00% | 0.00% |
| 6 | 1-A | 0.04 | 0.00% | 0.00% | 0.00% | 0.00% |

#### 6.2.2.3 Site Class C

For Site Class C, Table 6-10(a) shows that Regions 1 and 2 show relatively higher probabilities of exceeding the first limit state when a long lap-splice with non-seismic spacing is considered. However, when lap splice with seismic transverse reinforcement spacing is used, these probabilities drop down significantly from 24.60% to 10.78% for Region 1 and 16.03% to 6.22% for Region 2 as shown in Table 6-10(b). Hence, for Zone 1-B in Site Class B, it's recommended to use a lap splice with seismic reinforcement spacing, however, for Zone 1-A, long lap splice with non-seismic spacing could be used.

**Table 6-10 – Seismic Risk for MSC Supported Steel Bridges for Site Class C when (a) Lap-Splice with Non-Seismic Spacing is Provided, (b) Lap-Splice with Seismic Spacing is Provided, and (c) No Lap Splice is Provided.**

| Region | Zone | PGA (g) | Limit State 1 | Limit State 2 | Limit State 3 | Limit State 4 |
|---|---|---|---|---|---|---|
| 1 | 1-B | 0.19 | 24.60% | 4.02% | 1.81% | 0.45% |
| 2 | 1-B | 0.17 | 16.03% | 1.95% | 0.01% | 0.00% |
| 3 | 1-A | 0.12 | 3.92% | 0.21% | 0.09% | 0.01% |
| 4 | 1-A | 0.10 | 1.17% | 0.03% | 0.01% | 0.00% |
| 5 | 1-A | 0.07 | 0.17% | 0.00% | 0.00% | 0.00% |
| 6 | 1-A | 0.05 | 0.00% | 0.00% | 0.00% | 0.00% |

| Region | Zone | PGA (g) | Limit State 1 | Limit State 2 | Limit State 3 | Limit State 4 |
|---|---|---|---|---|---|---|
| 1 | 1-B | 0.19 | 10.78% | 0.56% | 0.09% | 0.04% |
| 2 | 1-B | 0.17 | 6.22% | 0.22% | 0.03% | 0.01% |

6.2.2.4 Site Class D

Table 6-11(a) shows that Limit State 1 failure probabilities of 44.00% and 31.39% for Region 1 and 2, respectively, when a long lap splice with non-seismic spacing is used. Table 6-11(b) shows the failure probabilities when no lap splice is used for Zone 2 and when lap splice is within the plastic hinge region with seismic spacing for Zone 1-A. The probabilities shown in Table 6-11(b) are significantly lower than those in Table 6-11(a). Hence, it's recommended that for Site Class D, the lap splice shall be outside the plastic hinge region for Zone 2. However, for Zone 1-B, the lap splice could still be within the plastic hinge region if seismic spacing is provided.

**Table 6-11 – Seismic Risk for MSC Steel Bridges for Site Class C when (a) Lap-Splice with Non-Seismic Spacing is Provided, and (b) No Lap Splice is Provided.**

| Region | Zone | PGA (g) | Limit State 1 | Limit State 2 | Limit State 3 | Limit State 4 |
|---|---|---|---|---|---|---|
| 1 | 2 | 0.24 | 44.00% | 11.69% | 5.82% | 1.84% |
| 2 | 2 | 0.21 | 31.39% | 6.22% | 2.91% | 0.80% |
| 3 | 1-B | 0.16 | 13.47% | 1.46% | 0.62% | 0.13% |
| 4 | 1-B | 0.13 | 5.74% | 0.38% | 0.15% | 0.03% |
| 5 | 1-B | 0.09 | 1.17% | 0.03% | 0.01% | 0.00% |
| 6 | 1-A | 0.06 | 0.07% | 0.00% | 0.00% | 0.00% |

| Region | Zone | PGA (g) | Limit State 1 | Limit State 2 | Limit State 3 | Limit State 4 |
|---|---|---|---|---|---|---|
| 1 | 2 | 0.24 | 17.79% | 1.10% | 0.17% | 0.08% |
| 2 | 2 | 0.21 | 10.53% | 0.42% | 0.06% | 0.03% |
| 3 | 1-B | 0.16 | 4.99% | 0.15% | 0.02% | 0.01% |
| 4 | 1-B | 0.13 | 1.74% | 0.03% | 0.00% | 0.00% |
| 5 | 1-B | 0.09 | 17.79% | 1.10% | 0.17% | 0.08% |

#### 6.2.2.5 Site Class E

For Site Class E, the corresponding probabilities of exceeding various limit states when a long lap splice with non-seismic spacing are used are shown in Table 6-12(a). The maximum probability of failure happens to be for Region 1 and is equal to 75.14%. Except for Region 6, which falls in Zone 1-B, the probabilities for other regions are quite high. AASTHO LRFD seismic provisions doesn't recommend that a lap splice should be provided in Seismic Zone 2. Table 6-12(b) shows the probabilities of exceeding limit states when the lap splice is outside the plastic hinge region for Zone 2 and when it is within the

plastic hinge region with seismic spacing for Zone 1-B. As can be seen, there is about 30% reduction in the probabilities for Region 1, hence, it's recommended to put the lap splice outside the plastic hinge region for Zone 2 in Site Class E.

**Table 6-12 – Seismic Risk for MSC Steel Bridge Class for Site Class C when (a) Lap-Splice with Non-Seismic Spacing is Provided, and (b) No Lap Splice is Provided**

| Region | Zone | PGA (g) | Limit State 1 | Limit State 2 | Limit State 3 | Limit State 4 |
|---|---|---|---|---|---|---|
| 1 | 2 | 0.35 | 75.14% | 37.22% | 22.37% | 10.01% |
| 2 | 2 | 0.28 | 56.78% | 19.63% | 10.46% | 3.80% |
| 3 | 2 | 0.25 | 46.51% | 13.07% | 6.59% | 2.14% |
| 4 | 2 | 0.20 | 27.56% | 4.93% | 2.26% | 0.59% |
| 5 | 2 | 0.15 | 10.54% | 0.98% | 0.41% | 0.08% |
| 6 | 1-B | 0.10 | 1.48% | 0.05% | 0.02% | 0.00% |

| Region | Zone | PGA (g) | Limit State 1 | Limit State 2 | Limit State 3 | Limit State 4 |
|---|---|---|---|---|---|---|
| 1 | 2 | 0.35 | 45.94% | 7.61% | 1.66% | 0.95% |
| 2 | 2 | 0.28 | 27.28% | 2.51% | 0.44% | 0.23% |
| 3 | 2 | 0.25 | 19.51% | 1.31% | 0.21% | 0.10% |
| 4 | 2 | 0.2 | 8.66% | 0.30% | 0.04% | 0.02% |
| 5 | 2 | 0.15 | 2.22% | 0.03% | 0.00% | 0.00% |
| 6 | 1-B | 0.10 | 0.35% | 0.00% | 0.00% | 0.00% |

### *6.2.3 Multi-Span Simply Supported Steel Bridges*

Seismic analysis of this bridge class is done using the same set of ground motions and same lap splice cases as the previous bridge class. Fig 4.3 presents the seismic fragility curves for MSSS Steel bridge class. For easier comparison between the bridge classes and

lap splice cases, the probability values are also presented in Table 4-1 up to 0.35g at intervals of 0.05g. In general, this bridge class shows increased probabilities compared to the other two bridge classes discussed in previous sections. This can be attributed to the following two reasons:

1) The length of the lap splice for MSSS Steel bridges is 6.5 ft. whereas for MSSS Concrete bridges, it is 9 ft. A shorter lap splice means leads to a greater degradation in strength as explained Chapter 2 and hence, attracts more damage.

2) The superstructure mass of MSSS Steel bridge is more than MSSS Concrete bridge due to a wider deck in the former. This imposes more demand on the columns, thus resulting in higher probabilities of reaching damage states.

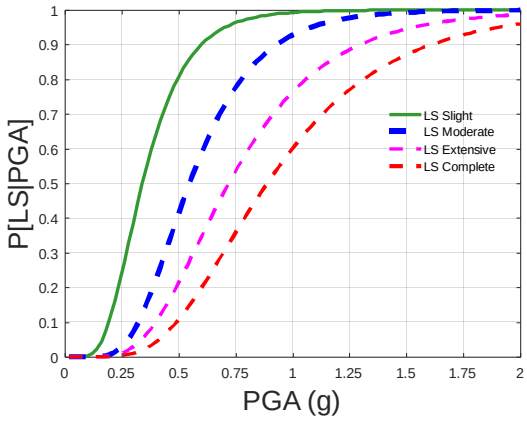


**Figure 6.4 (a)**

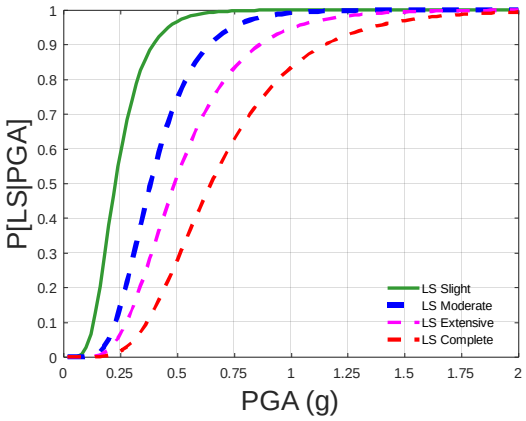


**Figure 6.4(b)**

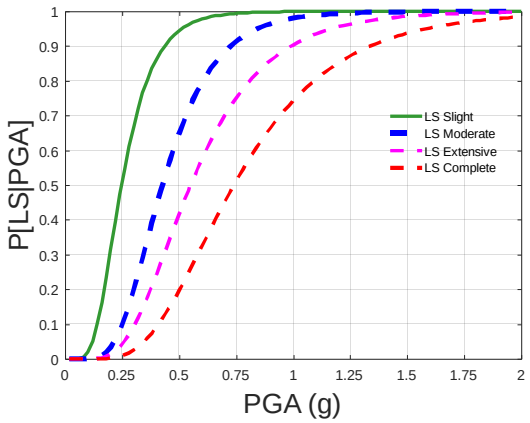


**Figure 6.4 (c)**

**Figure 6.4 - Seismic Fragility Curves for MSSS Steel Bridges for (a) No-Lap Splice with Seismic Spacing (s = 3 in.), (b) Lap Splice with Seismic Spacing (s = 3 in.), and (c) Lap Splice with Seismic Spacing (s = 12 in.).**

**Table 6-13 – Comparative Probability Estimates of Exceeding Four Limit States for MSSS Steel Bridges for (a) No-Lap Splice with Seismic Spacing (s = 3 in.), (b) Lap Splice with Seismic Spacing (s = 3 in.), and (c) Lap Splice with Seismic Spacing (s = 12 in.).**

**Table 6-13(a)**

| PGA (g) | LS 1 | LS 2 | LS 3 | LS 4 |
|---|---|---|---|---|
| 0.05 | 0.0% | 0.0% | 0.0% | 0.0% |
| 0.10 | 1.7% | 0.0% | 0.0% | 0.0% |
| 0.15 | 6.4% | 0.2% | 0.1% | 0.0% |
| 0.20 | 13.6% | 0.85% | 0.31% | 0.07% |
| 0.25 | 22.1% | 2.10% | 0.77% | 0.20% |
| 0.30 | 30.9% | 4.07% | 1.52% | 0.44% |
| 0.35 | 39.4% | 6.7% | 2.6% | 0.8% |

**Table 6-13(b)**

| PGA (g) | LS 1 | LS 2 | LS 3 | LS 4 |
|---|---|---|---|---|
| 0.05 | 0.9% | 0.0% | 0.0% | 0.0% |
| 0.10 | 9.2% | 0.2% | 0.1% | 0.0% |
| 0.15 | 23.6% | 1.5% | 0.6% | 0.0% |
| 0.20 | 38.8% | 4.4% | 1.8% | 0.3% |
| 0.25 | 52.0% | 8.9% | 3.7% | 0.7% |
| 0.30 | 62.8% | 14.8% | 6.4% | 1.5% |
| 0.35 | 71.1% | 21.2% | 9.7% | 2.5% |

**Table 6-13(c)**

| PGA (g) | LS 1 | LS 2 | LS 3 | LS 4 |
|---|---|---|---|---|
| 0.05 | 0.0% | 0.0% | 0.0% | 0.0% |
| 0.10 | 0.2% | 0.0% | 0.0% | 0.0% |
| 0.15 | 2.2% | 0.0% | 0.0% | 0.0% |
| 0.20 | 8.7% | 0.3% | 0.0% | 0.0% |
| 0.25 | 19.5% | 1.3% | 0.2% | 0.1% |
| 0.30 | 32.7% | 3.6% | 0.7% | 0.4% |
| 0.35 | 45.9% | 7.6% | 1.6% | 0.9% |

6.2.3.1 Site Class A

For MSSS steel bridges, as all the regions for Site Class A experience very low earthquake intensities, the risk estimates are within the acceptable range as shown in Table 6-14. Thus, the lap splice can be provided at the base with non-seismic spacing.

**Table 6-14 – Seismic Risk for MSSS Steel Bridges for Site Class A when Lap-Splice with Non-Seismic Spacing is Provided.**

| Region | Zone | PGA (g) | Limit State 1 | Limit State 2 | Limit State 3 | Limit State 4 |
|---|---|---|---|---|---|---|
| 1 | 1-A | 0.13 | 8.79% | 0.31% | 0.12% | 0.01% |
| 2 | 1-A | 0.11 | 4.77% | 0.11% | 0.04% | 0.00% |
| 3 | 1-A | 0.08 | 0.70% | 0.00% | 0.00% | 0.00% |
| 4 | 1-A | 0.06 | 0.14% | 0.00% | 0.00% | 0.00% |
| 5 | 1-A | 0.05 | 0.01% | 0.00% | 0.00% | 0.00% |
| 6 | 1-A | 0.03 | 0.00% | 0.00% | 0.00% | 0.00% |

#### 6.2.3.2 Site Class B

For Site Class B, even though all the regions fall in Zone 1-A, Table 6-15(a) shows that Regions 1 and 2 show high probabilities of exceeding Limit State 1 when non-seismic spacing is provided. As per Table 6-15(b), even when seismic spacing is provided, the probabilities tend to be on the higher side. On the other hand, elimination of lap splice from the column base leads to reduction of 15.96% for Region 1 and 10.43% for Region 2. Thus, it's recommended that for MSSS steel bridges, lap splice should not be provided at the base of the column for northern regions of Georgia (Regions 1 and 2) for Site Class B.

**Table 6-15 – Seismic Risk for MSSS Steel Bridges for Site Class B when (a) Lap-Splice with Non-Seismic Spacing is Provided, (b) Lap-Splice with Seismic Spacing is Provided, and (c) No Lap Splice is Provided.**

| Region | Zone | PGA (g) | Limit State 1 | Limit State 2 | Limit State 3 | Limit State 4 |
|---|---|---|---|---|---|---|
| 1 | 1-A | 0.16 | 20.30% | 1.47% | 0.58% | 0.08% |
| 2 | 1-A | 0.14 | 12.63% | 0.60% | 0.23% | 0.03% |
| 3 | 1-A | 0.10 | 2.66% | 0.04% | 0.02% | 0.00% |
| 4 | 1-A | 0.08 | 0.70% | 0.00% | 0.00% | 0.00% |
| 5 | 1-A | 0.06 | 0.09% | 0.00% | 0.00% | 0.00% |
| 6 | 1-A | 0.04 | 0.00% | 0.00% | 0.00% | 0.00% |

| Region | Zone | PGA (g) | Limit State 1 | Limit State 2 | Limit State 3 | Limit State 4 |
|---|---|---|---|---|---|---|
| 1 | 1-A | 0.16 | 16.16% | 0.90% | 0.35% | 0.05% |
| 2 | 1-A | 0.14 | 9.84% | 0.36% | 0.14% | 0.02% |

| Region | Zone | PGA (g) | Limit State 1 | Limit State 2 | Limit State 3 | Limit State 4 |
|---|---|---|---|---|---|---|
| 1 | 1-A | 0.16 | 4.34% | 0.14% | 0.05% | 0.01% |
| 2 | 1-A | 0.14 | 2.20% | 0.05% | 0.02% | 0.00% |

6.2.3.3 Site Class C

Like Site Class B, Regions 1 & 2 show very high probabilities of exceeding Limit State 1 as shown in Table 6-16(a). Regions 1 & 2 for Site Class C fall in Seismic Zone 1-B, however, Table 6-16(b) shows that providing seismic transverse spacing again doesn't reduce the percentages either. However, eliminating the lap splice at the base of the column

leads to reduction of 24.63% for Region 1 and 18.22% for Region 2 in terms of risk estimates. Hence, not providing a lap splice at the bottom base seems to be the best option for Site Class C as well as can be seen from Table 6-16(c).

**Table 6-16 – Seismic Risk for MSSS Steel Bridges for Site Class C when (a) Lap-Splice with Non-Seismic Spacing is Provided, (b) Lap-Splice with Seismic Spacing is Provided, and (c) No Lap Splice is Provided.**

| Region | Zone | PGA (g) | Limit State 1 | Limit State 2 | Limit State 3 | Limit State 4 |
|---|---|---|---|---|---|---|
| 1 | 1-B | 0.19 | 34.33% | 4.24% | 1.73% | 0.31% |
| 2 | 1-B | 0.17 | 23.68% | 1.99% | 0.79% | 0.12% |
| 3 | 1-A | 0.12 | 6.61% | 0.19% | 0.07% | 0.01% |
| 4 | 1-A | 0.10 | 2.13% | 0.03% | 0.01% | 0.00% |
| 5 | 1-A | 0.07 | 0.34% | 0.00% | 0.00% | 0.00% |
| 6 | 1-A | 0.05 | 0.01% | 0.00% | 0.00% | 0.00% |

| Region | Zone | PGA (g) | Limit State 1 | Limit State 2 | Limit State 3 | Limit State 4 |
|---|---|---|---|---|---|---|
| 1 | 1-B | 0.19 | 28.29% | 2.72% | 1.08% | 0.17% |
| 2 | 1-B | 0.17 | 19.02% | 1.24% | 0.48% | 0.07% |

| Region | Zone | PGA (g) | Limit State 1 | Limit State 2 | Limit State 3 | Limit State 4 |
|---|---|---|---|---|---|---|
| 1 | 1-B | 0.19 | 9.70% | 0.55% | 0.20% | 0.05% |
| 2 | 1-B | 0.17 | 5.46% | 0.21% | 0.08% | 0.02% |

6.2.3.4 Site Class D

For Site Class D, Table 6-17(a) shows that Regions 4, 5, and 6 fall within a safe range when non-seismic spacing is provided. However, as most of the northern region of

the state lies in Zone 2 (except Region 4), the lap splice shouldn't be provided at the base of the columns as per the AASHTO Design Specifications. The advantage of eliminating the lap splice when the bridge lies in Seismic Zone 2 can also be observed from Table 6-17(b) where exclusion of the lap splice leads to a maximum reduction in damage risk probability of about 33.71% for Region 1.

**Table 6-17 – Seismic Risk for MSSS Steel Bridges for Site Class C when (a) Lap-Splice with Non-Seismic Spacing is Provided, and (b) No Lap Splice is Provided.**

| Region | Zone | PGA (g) | Limit State 1 | Limit State 2 | Limit State 3 | Limit State 4 |
|---|---|---|---|---|---|---|
| 1 | 2 | 0.24 | 55.92% | 12.79% | 5.69% | 1.37% |
| 2 | 2 | 0.21 | 42.33% | 6.68% | 2.80% | 0.57% |
| 3 | 1-B | 0.16 | 20.30% | 1.47% | 0.58% | 0.08% |
| 4 | 1-B | 0.13 | 9.38% | 0.35% | 0.14% | 0.02% |
| 5 | 1-B | 0.09 | 2.13% | 0.03% | 0.01% | 0.00% |
| 6 | 1-A | 0.06 | 0.14% | 0.00% | 0.00% | 0.00% |

| Region | Zone | PGA (g) | Limit State 1 | Limit State 2 | Limit State 3 | Limit State 4 |
|---|---|---|---|---|---|---|
| 1 | 2 | 0.24 | 22.21% | 2.44% | 0.91% | 0.26% |
| 2 | 2 | 0.21 | 13.66% | 1.01% | 0.37% | 0.09% |
| 3 | 1-B | 0.16 | 4.34% | 0.14% | 0.05% | 0.01% |

6.2.3.5 Site Class E

For Site Class E, most of the state falls in Seismic Zone 2. AASTHO LRFD Design Specifications doesn't recommend providing a lap splice at the column base for Seismic Zone 2 and this is evident from Table 6-18(a) as the probabilities are very high. Hence, to

be on the safer side, no lap splice should be provided at the base of the columns as this reduces the percentages considerably as shown in Table 6-18(b).

**Table 6-18 – Seismic Risk for MSSS Steel Bridges for Site Class C when (a) Lap-Splice with Non-Seismic Spacing is Provided, and (b) No Lap Splice is Provided**

| Region | Zone | PGA (g) | Limit State 1 | Limit State 2 | Limit State 3 | Limit State 4 |
|---|---|---|---|---|---|---|
| 1 | 2 | 0.35 | 84.24% | 40.98% | 22.44% | 8.27% |
| 2 | 2 | 0.28 | 68.48% | 21.66% | 10.36% | 2.95% |
| 3 | 2 | 0.25 | 58.53% | 14.32% | 6.46% | 1.61% |
| 4 | 2 | 0.20 | 37.91% | 5.25% | 2.16% | 0.41% |
| 5 | 2 | 0.15 | 16.30% | 0.97% | 0.38% | 0.05% |
| 6 | 1-B | 0.10 | 2.66% | 0.04% | 0.02% | 0.00% |

| Region | Zone | PGA (g) | Limit State 1 | Limit State 2 | Limit State 3 | Limit State 4 |
|---|---|---|---|---|---|---|
| 1 | 2 | 0.35 | 52.46% | 13.87% | 5.86% | 2.22% |
| 2 | 2 | 0.28 | 32.85% | 5.19% | 2.01% | 0.64% |
| 3 | 2 | 0.25 | 24.17% | 2.86% | 1.08% | 0.31% |
| 4 | 2 | 0.2 | 11.38% | 0.73% | 0.27% | 0.06% |
| 5 | 2 | 0.15 | 3.16% | 0.08% | 0.03% | 0.01% |

# CHAPTER 7. CONCLUSIONS, KEY CONTRIBUTIONS AND FUTURE WORK

## 7.1 Summary and Key Contributions

Because the state of Georgia is identified as a region with low-to-moderate seismic activity, non-seismically designed bridges have been a traditional bridge design practice in the state. However, recent studies revealed the need to consider seismic hazard in design of structures for bridges in Georgia. This led to adoption of seismic provisions from AASHTO LRFD Bridge Design Specifications into the Georgia DOT's Bridge and Structure Design Manual. This study presents the impact of latest seismic detailing requirements on previously built bridge columns in Georgia. Based on the results, recommendations on seismic design of columns for various bridge and site classes are provided to GDOT.

The first part of the study focuses on the literature review on the previous research done on lap splices highlighting the importance of providing adequate lap splice length and transverse reinforcement to increase strength and ductility of columns, especially in the case of cyclic loading. Further, a lap splice force transfer mechanism used in the study is presented. The lap splice model based on this mechanism depends on various factors, such as the length of the lap splice, the transverse reinforcement spacing, the steel strength and the steel rebar diameter. A parametric study investigating the impact of these variables on the lap splice stress-strain is conducted to determine the extent of influence of the factors.

To study the impact of the latest AASHTO LRFD Bridge Design Specifications, it is necessary to identify the potential seismic hazard in the state of Georgia. This is accomplished by dividing the state into six regions based on maximum PGA for Site Classes A, B, C, D and E. It is found that the northern region of Georgia for each site class is most susceptible to potential earthquakes. The maximum PGA in the state is expected for Site Class E in the northern region of Georgia and is equal to 0.35g.

The lap splice model along with the variation of transverse reinforcement spacing is incorporated into the 3-D finite element models on OpenSees. These models are used to estimate the demand imposed on bridge columns through running nonlinear time history analyses. Four classes of highway bridges, namely multi-span simply supported (MSSS) concrete girder bridges, multi-span continuous (MSC) steel girder bridges, MSSS steel girder bridges, and MSSS slab bridges, are analysed to evaluate their fragility. The ground motion for the deterministic analysis is chosen such that its maximum acceleration matches the expected peak ground acceleration (PGA) in Georgia. The deterministic nonlinear time history analyses reveal the deficiency in the column response and increase in the curvature demand when a lap splice is provided with non-seismic detailing for the northern regions of Georgia. Because the chosen ground motion is of moderate PGA, the bearing response in all the cases is similar.

The representative bridge from each bridge class is analysed probabilistically using a suite of 48 ground motions in order to account for seismic uncertainty. The capacity and demand imposed on the columns are compared in terms of curvature ductility to evaluate their damage risk estimates. Following are the main conclusions drawn from the probabilistic analyses:

1. For MSSS concrete girder bridges, it is recommended that 6.5’ lap splice can be provided at the base of the columns with 12” spacing for Seismic Zone 1-A irrespective of the site class. Although for Site Class B, the northern most region of the state with a PGA equal to 0.16g falls in Seismic Zone 1-A, a spacing of 3” could be used to be on the conservative side as the probability of exceedance of the Limit State 1 is 13.83% (refer to Sections 6.2.1.1 and 6.2.1.2).

   Regions 1 and 2 with PGA 0.19g and 0.17g, respectively, for Site Class C and Region 3 with PGA 0.16g for Site Class D fall in Seismic Zone 1-B. Hence, it is recommended that the 6.5’ lap splice can be used at the bottom of columns with 3” seismic spacing (refer to Sections 6.2.1.3 and 6.2.1.4).

   For Seismic Zone 2, the lap splice should not be provided at the base of the column irrespective of the site class (refer to Section 6.2.1.5).

2. For MSC steel girder bridges, it is recommended that 9’ lap splice can be provided at the base of the columns with 12” spacing for Seismic Zone 1-A irrespective of the site class. Although for Site Class B, the northern most region of the state with a PGA equal to 0.16g falls in Seismic Zone 1-A, a spacing of 3” could be used to be on the conservative side as the probability of exceedance of the Limit State 1 is 13.50% (refer to Sections 6.2.2.1, 6.2.2.2 and 6.2.2.3).

   For Seismic Zone 1-B, the 9’ lap splice could be provided at the base of the column with transverse reinforcement spacing equal to 3” (refer to Sections 6.2.2.4 and 6.2.2.5).

   Similar to the previous bridge class, for Seismic Zone 2, the lap splice should not be provided at the base of the column irrespective of the site class (refer to Section 6.2.2.5).

3. For MSSS steel girder bridges, Site Class A does not require attention towards seismic design as the probability ranges are within the acceptable range (refer to Section 6.2.3.1). However, for every other site class, lap splice should not be provided at the base of the columns for northern regions of Georgia (Regions 1 & 2) (refer to Sections 6.2.3.2, 6.2.3.3, 6.2.3.4 and 6.2.3.5). Additionally, for Site Class D, as most of the state falls in Seismic Zone 1-B, it is recommended that the 6.5' lap splice must only be provided with 3" transverse spacing to be on the conservative side (refer to Section 6.2.3.4). Most of the state for Site Class E falls in Seismic Zone 2; hence, it is recommended that the lap splice should not be provided at the base of the columns for this site class (refer to Section 6.2.3.5).
4. For multi-span simply supported (MSSS) slab bridges, the conventional practice is to support the bridge superstructure on piles. The pile-bent connection is created such that the pile is embedded into the bent cap up to a certain depth depending on the diameter of the pile. In Georgia, the typical practice is to extend the pile 1 ft. into the cap if the pile diameter is 24 in. or less. For wider piles, the embedment depth is usually increased to 1.5 ft. to 2 ft.

   The state of South Carolina also follows the same pile-bent connection type; however, the embedment length is detailed differently from Georgia. In South Carolina, the embedment length should be equal to pile cross-section dimension (SC DOT, 2006).

   Section 10.7.1.2 in the latest AASTHO LRFD Design Specifications (2014) suggests that the pile should at least extend 12 in. into the cap. Additionally, according to Section 5.13.4.6.2 of the Specifications, for Seismic Zone 2, piles shall be used to resist both axial and lateral loads. The minimum depth of embedment and axial and

lateral pile resistances required for seismic loads shall be determined by the means of design criteria established by site-specific geological and geotechnical investigations. Dowel bars designed as per the development length criterion must be provided between the pile and bent to develop uplift forces.

## 7.2 Future Work

Potential areas for future studies could be as follows:

1. The present study that the soil and foundation properties at the column bases and abutments are same for every site class due to unavailability of the soil property data in the state of Georgia. Future studies could evaluate the impact of soil properties related to different site classes on the expected performance of bridges and corresponding damage risk.
2. All uncertainty parameters except seismic hazard are ignored in this study. The representative bridge for each bridge class is selected such that its characteristics are close to the median of the bridge class obtained from inventory analysis of Georgia highway bridges. To obtain more accurate fragility estimates, other factors of uncertainty such as material properties, geometric properties, etc. could be included in the future studies.
3. The present study uses the truss-based lap splice model to investigate the expected performance of bridge columns. Another popular model based on the bond slip mechanism could also be used to evaluate the same. Additionally, response of various other splicing techniques such as welding, couplers, mechanical splices could also be investigated.

4. The study focussed on analysis of old bridges in Georgia, however, any kind of deterioration mechanisms that may play a part in strength degradation of these bridges were not considered. Considering these factors might lead to additional demand on columns and hence, stricter seismic guidelines.

# REFERENCES


AASHTO. 2014. *AASHTO LRFD Bridge Design Specifications*. American Association of State Highway and Transportation Officials, Washington, D.C.

Abdel-Kareem, AH, and H Abousafa. 2013. "Effect of Transverse Reinforcement on the Behavior of Tension Lap Splice in High-Strength Reinforced Concrete Beams." *World Academy of Science,*.

Aboutaha, Riyad S., Michael U. Engelhardt, James O. Jirsa, and Michael F. Kreger. 1996. "Retrofit of Concrete Columns with Inadequate Lap Splices by the Use of Rectangular Steel Jackets." *Earthquake Spectra* 12 (4): 693–714. doi:10.1193/1.1585906.

Basoz, Nesrin, and Anne S. Kiremidjian. 1999. "Development of Empirical Fragility Curves for Bridges." *Technical Council on Lifeline Earthquake Engineering Monograph*, no. 16. ASCE: 693–702.

Biryol, C. Berk, Lara S. Wagner, Karen M. Fischer, and Robert B. Hawman. 2016. "Relationship between Observed Upper Mantle Structures and Recent Tectonic Activity across the Southeastern United States." *Journal of Geophysical Research: Solid Earth* 121 (5): 3393–3414. doi:10.1002/2015JB012698.

Biskinis, Dionysis, and Michael N. Fardis. 2007. "Effect of Lap Splices on Flexural Resistance and Cyclic Deformation Capacity of RC Members." *Beton- Und Stahlbetonbau* 102 (S1). WILEY-VCH Verlag: 51–59. doi:10.1002/best.200710105.

Cairns, J ., and P. D. Arthur. 1979. "Strength of Lapped Splices in Reinforced Concrete Columns." *ACI Journal Proceedings* 76 (2): 277–96. doi:10.14359/6947.

Calderone, Anthony. 2001. *Behavior of Reinforced Concrete Bridge Columns Having Varying Aspect Ratios and Varying Lengths of Confinement /*. Berkeley : Pacific Earthquake Engineering Research Center,.

Canbay, E, and RJ Frosch. 2005. "Bond Strength of Lap-Spliced Bars." *ACI Structural Journal*.

ChaiI, Yuk Hon, M. J. Nigel Priestley, and Frieder Seible. 1991. "Seismic Retrofit of Circular Bridge Columns for Enhanced Flexural Performance." *ACI Structural*

*Journal* 88 (5): 572–84. doi:10.14359/2759.

Cho, JY, and JA Pincheira. 2004. “Nonlinear Modeling of RC Columns with Short Lap Splices.” *13 WCEE: 13 Th World Conference on Earthquake*.

Choi, Eunsoo. 2002. “Seismic Analysis and Retrofit of Mid-America Bridges.” Georgia Institute of Technology.

Cornell, C. Allin, Fatemeh Jalayer, Ronald O. Hamburger, and Douglas A. Foutch. 2002. “Probabilistic Basis for 2000 SAC Federal Emergency Management Agency Steel Moment Frame Guidelines.” *Journal of Structural Engineering* 128 (4): 526–33. doi:10.1061/(ASCE)0733-9445(2002)128:4(526).

El-Azab, Mahmoud A., Hatem M. Mohamed, and Ahmed Farahat. 2014. “Effect of Tension Lap Splice on the Behavior of High Strength Self-Compacted Concrete Beams.” *Alexandria Engineering Journal* 53 (2): 319–28. doi:10.1016/j.aej.2014.01.009.

FEMA. 2003. “HAZUS. Earthquake Model, Technical Manual, Federal Emergency Management Agency.” Washington DC.

FHWA. 2002. “National Bridge Inventory.”

Freytag, DM. 2006. “Bar Buckling in Reinforced Concrete Bridge Columns.”

Georgia DOT (GDOT). 2017. “Georgia Department of Transportation Bridge and Structures Design Manual,” no. OCTOBER 2005.

Ghosh, J, and JE Padgett. 2010. “Aging Considerations in the Development of Time-Dependent Seismic Fragility Curves.” *Journal of Structural Engineering*.

Ghosh, Jayadipta. 2013. “Parameterized Seismic Reliability Assessment and Life-Cycle Analysis of Aging Highway Bridges.” Rice University, Houston, Texas.

Hamad, B. S., and S. Najjar. 2002. “Evaluation of the Role of Transverse Reinforcement in Confining Tension Lap Splices in High Strength Concrete.” *Materials and Structures* 35 (4). Kluwer Academic Publishers: 219–28. doi:10.1007/BF02533083.

Hannewald, Pia. 2013. “Seismic Behavior of Poorly Detailed RC Bridge Piers.” *PhD Thesis, École Polytechnique Fédérale de Lausanne*.

Harajli, MH, BS Hamad, and AA Rteil. 2005. “Effect of Confinement on Bond Strength between Steel Bars and Concrete"(vol 101, Pg 595, 2004).” *ACI*.

Harajli, Mohamed H., and Farid Dagher. 2008. “Seismic Strengthening of Bond-Critical Regions in Rectangular Reinforced Concrete Columns Using Fiber-Reinforced Polymer Wraps.” *ACI Structural Journal* 105 (1): 68–77. doi:10.14359/19070.

Hite, MC. 2007. “Evaluation of the Performance of Bridge Steel Pedestals under Low Seismic Loads.”

Illinois DOT (IDOT). 2009. *Bridge Manual*. IDOT, Springfield, IL.

Jaradat, Omar A., David I. McLean, and M. Lee Marsh. 1998. “Performance of Existing Bridge Columns under Cyclic Loading - Part 1: Experimental Results and Observed Behavior.” *ACI Structural Journal* 95 (6): 695–704.

Kiureghian, A Der. 2002. “Bayesian Methods for Seismic Fragility Assessment of Lifeline Components.” *Acceptable Risk Processes–Lifelines and*.

Lehman, DE. 2000. “Seismic Performance of Well-Confined Concrete Bridge Columns.”

Lin, Yongqian, and Neil M. Hawkins. 1996. *Seismic Behavior of Bridge Pier Column Lap Splices*.

Lynn, AC, JP Moehle, and SA Mahin. 1996. “Seismic Evaluation of Existing Reinforced Concrete Building Columns.” *Earthquake*.

Mabrouk, Rasha T.S., and Ahmed Mounir. 2017. “Behavior of RC Beams with Tension Lap Splices Confined with Transverse Reinforcement Using Different Types of Concrete under Pure Bending.” *Alexandria Engineering Journal*. doi:10.1016/j.aej.2017.05.001.

MacKay, B., D. Schmidt, and T. Rezansoff. 1989. “Effectiveness of Concrete Confinement on Lap Splice Performance in Concrete Beams under Reversed Inelastic Loading.” *Canadian Journal of Civil Engineering* 16 (1). NRC Research Press Ottawa, Canada

: 36–44. doi:10.1139/l89-005.

Mander, JB, DK Kim, SS Chen, and GJ Premus. 1996. “Response of Steel Bridge Bearings to Reversed Cyclic Loading.”

Mander, JB, MJN Priestley, and R Park. 1988. “Theoretical Stress-Strain Model for Confined Concrete.” *Journal of Structural*.

Mander, John B, and Nesrin Basöz. 1999. “Seismic Fragility Curve Theory for Highway Bridges.” In *Technical Council on Lifeline Earthquake Engineering Monograph Proceedings of the 1999 5th US Conference on Lifeline Earthquake Engineering Optimazing PostEarthquake Lifeline System Reliability*, 31–40. ASCE.

Mazzoni, Silvia, Frank Mckenna, Michael H Scott, and Gregory L Fenves. 2006. “Open System for Earthquake Engineering Simulation (OpenSees) OpenSees Command Language Manual.”

Melek, Murat, and John W. Wallace. 2004. “Cyclic Behavior of Columns with Short Lap Splices.” *ACI Structural Journal* 101 (6): 802–11. doi:10.14359/13455.

Mylonakis, G, C Syngros, and G Gazetas. 2006. “The Role of Soil in the Collapse of 18 Piers of Hanshin Expressway in the Kobe Earthquake.” *Earthquake*.

Nielson, BG, and R DesRoches. 2007. “Analytical Seismic Fragility Curves for Typical Bridges in the Central and Southeastern United States.” *Earthquake Spectra*.

Nielson, Bryant G. 2005. “Analytical Fragility Curves for Highway Bridges in Moderate Seismic Zones.” *Environmental Engineering*. Georgia Institute of Technology. doi:10.1016/j.engstruct.2017.03.041.

Orangun, CO, JO Jirsa, and JE Breen. 1977. “A Reevaluation of Test Data on Development Length and Splices.” *ACI Journal*.

Paulay, T, TM Zanza, and A Scarpas. 1981. “Lapped Splices in Bridge Piers and in Columns of Earthquake Resisting Reinforced Concrete Frames.”

Paulay, Thomas. 1982. “Lapped Splices in Earthquake-Resisting Columns.” *ACI Journal Proceedings* 79 (6). doi:10.14359/10920.

Priestley, MJN, F Seible, and GM Calvi. 1996. *Seismic Design and Retrofit of Bridges*.

Rix, GJ, and JA Fernandez-Leon. 2004. "Synthetic Ground Motions for Memphis, TN." *Æ Http://www. Ce. Gatech. Edu/research/*.

Roeder, Charles W., and John F. Stanton. 1983. "Elastomeric Bearings: State?of?the?Art." *Journal of Structural Engineering* 109 (12): 2853–71. doi:10.1061/(ASCE)0733-9445(1983)109:12(2853).

Rojahn, C, and RL Sharpe. 1985. "Earthquake Damage Evaluation Data for California."

SC DOT. 2006. "SC DOT Bridge Design Manual."

Scharge, L. 1981. "Anchoring of Bearings by Friction, Joint Sealing and Bearing Systems for Concrete Structures." *World Congress on Joints and Bearings*.

Shinozuka, M, MQ Feng, H Kim, T Uzawa, and T Ueda. 2003. "Statistical Analysis of Fragility Curves. Report." *Multidisciplinary Center for*.

Sozen, MA, and JP Moehle. 1990. "Development and Lap-Splice Lengths for Deformed Reinforcing Bars in Concrete: A Report to the Portland Cement Association, Skokie, IL, and the."

Steelman, JS, ET Filipov, and LA Fahnestock. 2013. "Experimental Behavior of Steel Fixed Bearings and Implications for Seismic Bridge Response." *Journal of Bridge*.

Sun, Z, MJN Priestley, and F Seible. 1993. "Diagnostics and Retrofit of Rectangular Bridge Columns for Seismic Loads."

Tariverdilo, S., A. Farjadi, and M. Barkhordary. 2009. "Fragility Ccurves for Reinforced Concrete Frames With Lap-Spliced Columns." *International Journal of Engineering - Transactions A: Basics* 22 (3): 213.

Wu, Chenglin, Genda Chen, Jeffery S. Volz, Richard K. Brow, and Michael L. Koenigstein. 2013. "Global Bond Behavior of Enamel-Coated Rebar in Concrete Beams with Spliced Reinforcement." *Construction and Building Materials* 40 (March): 793–801. doi:10.1016/j.conbuildmat.2012.11.076.

Zhiqiang, Wang, and George C Lee. 2009. “A Comparative Study of Bridge Damage due to the Wenchuan, Northridge, Loma Prieta and San Fernando Earthquakes.” *Earthquake Eng & Eng Vib* 8 (8): 251–61. doi:10.1007/s11803-009-9063-y.